of *in vivo* nanoparticles in tumor targeting could be hampered by factors such as bio-incompatibility and opsonization, leading to the undesirable removal of nanoparticles by mononuclear phagocytotic cells [26]. Active targeting increases the affinity of the carrier system for the target site, while passive targeting minimizes the non-specific interaction with non-targeted sites by the reticuloendothelial systems (RES). However, gene transfer activity after intravenous injection of a cationic liposome / plasmid DNA complex is most prevalent in the lung [27]. The challenge for tumor-specific targeting using non-viral gene delivery systems is to decrease this non-specific gene transfer in the lung, while simultaneously maintaining or increasing the level of gene transfer to the tumor tissues. The liposomes used in recent studies have been coated with folate-polyethylene glycol (PEG)-lipid to facilitate tumor-targeting by an active mechanism (*via* FR) and a passive mechanism (prevention/reduction of RES uptake) [20,28]. PEGylated lipids can significantly reduce the non-specific gene transfer activity in lung, and conjugation of the targeting ligand, folate, to the PEG chain, can restore this activity in FR-positive tumors *in vivo* [20].

A schematic illustration of the FR-targeting concept is presented in Fig. 1. Long-circulating nanoparticles, such as PEG-coated nanoparticles, tend to accumulate in tumors as a result of increased microvascular permeability and defective lymphatic drainage, a process also referred to as the enhanced permeability and retention (EPR) effect [28]. This is a passive and non-specific process of extravasation that is statically improved by the prolonged residence time of nanoparticles in circulation and repeated passages through the tumor microvascular bed. For intra-vascular targeting to access tumor cells expressing FR, nanoparticles must cross the vascular endothelium and diffuse into the interstitial fluid [28]. The theoretical advantage of FR-targeting over non-targeting is related to a shift in the distribution of the nanoparticles to the tumor cell compartment and delivery of the gene. The disadvantage of a system targeting a cancer cell receptor such as FR, is the difficulty that a large nano-size assembly has in penetrating a solid tumor mass. The development of suitable delivery vectors for *in vivo* gene transfer is necessary for the clinical application of therapeutic genes.

Several cationic polymer-folate conjugates and/or cationic liposomes, and cationic nanoparticles incorporating folate-derivatives have been developed for FR-targeted gene delivery (Table 1). Folic acid retains its receptor-binding and endocytotic properties when covalently linked to a wide variety of molecules.

Polymers

Polyplexes are composed of charged complexes of plasmid DNA and a cationic polymer, such as poly-L-lysine (PLL), polyethylenimine (PEI) and polyamidoamine dendrimers. Cationic polymers and plasmid DNA can form condensed particles with a net positive charge. This protects the DNA from nuclease-mediated degradation and enables charge-mediated non-specific cellular association. For FR-

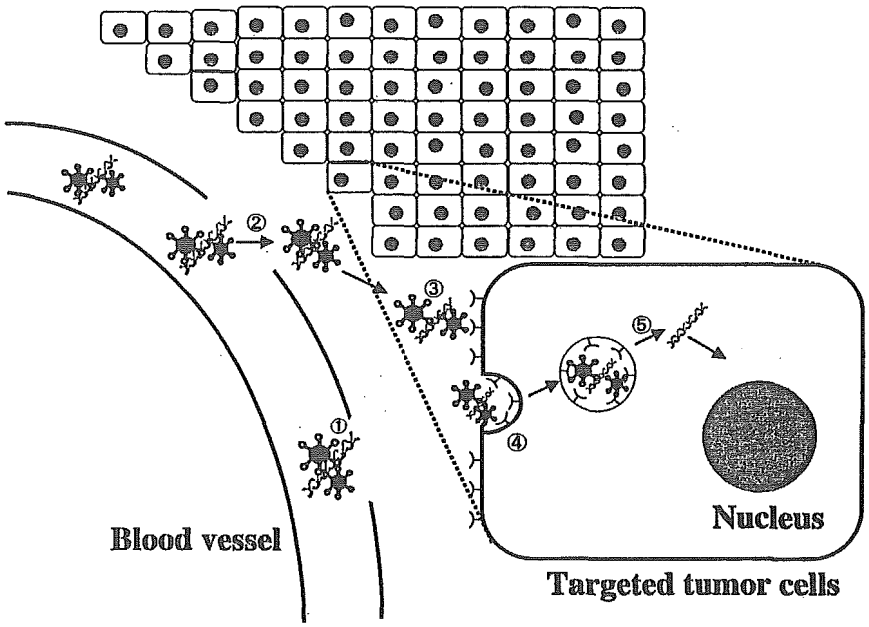

Fig. (1). Schematic drawing illustrating the concept of using FR-targeting nanoparticles to deliver plasmid DNA to tumor cells. The dots and helixes on the nanoparticles represent the folate ligands and plasmid DNA, respectively. The various steps involved in the targeting process are numbered from 1 to 5. Steps 1-2 are common to non-targeted and FR-targeting nanoparticles mixed with plasmid DNA (nanoplex). Steps 3-5 are specific to the FR-targeting vector. (1) long-circulating nanoplexes make more passages through the tumor microvasculature. (2) Increased vascular permeability in tumor tissue enables nanoplexes to extravasate and reach the tumor interstitial fluid. (3) FR-targeting nanoplexes bind to FR expressed on the tumor membrane *via* the folate ligand. (4) The nanoplexes are internalized by tumor cells *via* FR. (5) Internalized nanoplexes release their plasmid DNA in the cytoplasm.

Table 1. FR-Targeting Nonviral Vectors. All Vectors were used in *In Vitro* Transfection

Vector		Description	*In Vivo*	References
Polymer	Poly-L-Lys (PLL)	Polyplex prepared with PLL-folate or PLL-PEG_{3400}-folate	-	[29-32]
	Polyethylenimine (PEI)	Polyplex prepared with PEI-folate or PEI-PEG_{3350}-folate	-	[33,34]
	Polydimethylamino methylmethacrylate (pDMAEMA)	Polyplex prepared with pDMAEMA-PEG_{3400}-folate	-	[35]
Liposome	Cationic liposome	Incorporating 0.1 mol% folate-PEG_{3350}-DOPE, 5 mol% folate-DOPE, 0.5-5 mol% folate-PEG_{3400}-DSPE or 5 mol % folate-PEG_{4600}-cholesterol into liposome	i.v.	[15,17-20,36]
	LPDI type	Polyplex prepared from protamine was mixed with catonic liposome containing 0.3 mol% folate-PEG_{3400}-DSPE or 2 mol% folate-PEG_{5000}-DSPE	i.p. i.v.	[21,37]
	LPDII type	Polyplex prepared from PLL or PEI was mixed with pH-sensitive anionic liposome containing 0.1 mol% folate-PEG_{3350}-DOPE or folate-PEG_{3350}-DSPE	-	[16,38]
Nanoparticle		Polyplex prepared with cationic dithiol-detergent ($(C_{14}Com)_2$) was mixed with 2 mol% folate-PEG_{3400}-DPPE	-	[39]
	NP-F	Incorporating 2 mol% folate-PEG_{2000}-DSPE into cationic nanoparticle	i.v. i.t.	[40,41]

i.v.: intravenous injection, i.p.: intraperitoneal injection; i.t.: intratumoral injection

targeted gene delivery, PLL-folate [29-31], PLL-PEG-folate [32], PEI-folate [33], PEI-PEG-folate [33,34], and poly(dimethylaminomethyl methacrylate) (pDMAEMA)-PEG-folate [35] have been synthesized. These folate-conjugates facilitated efficient FR-targeted gene delivery without additional vector components *in vitro*. It appears that the incorporation of a long PEG spacer between folate and the cationic polymer is important for efficient FR-targeted gene delivery [31].

Liposomes

Lipoplexes are composed of charge complexes of plasmid DNA and cationic liposome. Lipopolyplexes are composed of plasmid DNA attached to both polymers and lipids. Cationic liposomes are generally composed of a cationic lipid, such as dioleoyltrimethylammonium chloride (DOTMA), dioleoyltrimethylammonium propane (DOTAP), or dimethylaminoethanolamine carbamoyl cholesterol (DC-Chol), and a helper lipid, such as DOPE or cholesterol (Chol), which provides fusogenicity and stability to the lipoplex. Depending on the preparation, the lipoplex may not be a single aggregate, but an intricate structure in which the condensed DNA is surrounded by a lipid bilayer. FR-targeting cationic liposomes were incorporated with folate-derivatives, folate-DOPE [36], folate-PEG-DOPE [15,16], folate-PEG-DSPE [17-21,37], folate-PEG-Chol [20], etc. Hofland *et al.*[20] showed that both folate-PEG_{3400}-DSPE and folate-PEG_{4600}-Chol, when combined with a cationic lipid RPR209120 and DOPE, formed lipoplexes with greatly reduced normal tissue gene transfer and efficient *in vivo* tumor gene transfer.

LPDI-type lipoplexes (lipopolyplex) consist of a ternary complex of cationic liposomes, DNA-condensing polycation, and plasmid DNA. In a report by Reddy *et al.* [21], polyplexes prepared from protamine were mixed with cationic liposomes containing folate-PEG_{3400}-DSPE as a targeting ligand and DOPE as a helper lipid. This vector showed superior transfection activity in FR-positive M109 murine lung carcinoma cells as well as in ascitic cells derived from L1210A murine lymphocytic leukemia cells. LPDII-type lipoplexes (lipopolyplex) consist of a ternary complex of anionic liposomes, DNA-condensing polycation, and plasmid DNA. Lee *et al.* [16] reported a formulation of LPDII-type vector, in which DNA was first attached to PLL and then mixed with pH-sensitive anionic liposomes composed of DOPE/CHEMS/folate-PEG_{3350}-DOPE. PH-sensitive liposomes are fusogenic at acidic pH, and thus can be used to facilitate the endosomal disruption and subsequent release of plasmids in the cytoplasm. Shi *et al.* [38] reported efficient gene delivery using an LPDII vector that incorporated PEI as a DNA-condensing agent and a cationic/anionic lipid pair, composed of dimethyldioctadecylammonium bromide (DDAB)/CHEMS/polyoxyethylene sorbitan monooleate (Tween80)/folate-PEG_{3350}-DSPE.

Nanoparticles

Nanoplexes are composed of charged complexes of plasmid DNA and cationic nanoparticles. Here the definition of a lipid-based nanoparticle is a formula containing no bilayers like liposomes. Dauty *et al.* [39] reported that an FR-targeting cationic nanoparticle incorporating folate-PEG_{3400}-DPPE and a cationic dithiol-detergent (dimerized tetradecyl-ornithinyl-cysteine, $(C14Corn)_2$) showed efficient FR-dependent cellular uptake and transfection. In our laboratory, folate-linked nanoparticles, NP, NP-1F, -2F and -3F, consisting of 1 mg/ml DC-Chol as a cationic lipid, 5 mol%

Tween 80, and 0, 1, 2 and 3 mol% folate-PEG_{2000}-DSPE, respectively, were prepared by a modified ethanol injection method [40,41]. Cholesterol derivatives are usually unable to form stable bilayers, unless used in combination with DOPE or some other neutral lipid. Therefore, these particles may be nanoparticles. Folate-linked nanoparticles are illustrated in (Fig. 2). The average size of each nanoparticle was about 100-200 nm (Table 2). The ζ-potential of NP, NP-1F and -2F was about 53, 44 and 39 mV, respectively, decreasing as the amount of folate-PEG_{2000}-DSPE added increased, except for NP-3F [41].

When the nanoparticles were mixed with DNA at the optimal charge ratio (+/-) of cationic nanoparticle to DNA (3/1), the size of each nanoplex increased from 200 to 500 nm, and the ζ-potential slightly decreased to +40 ~ +30 mV (Table 2). In the presence of 10% and 50% serum, the NP-2F nanoplexes did not increase greatly in size and remained injectable. NP-2F showed high gene transfection *in vivo* as mentioned below.

Many cell types, including most tumor cells, display a low endocytotic capacity. Since the intracellular mechanism of FR-targeted gene delivery with liposomes and nanoparticles is endocytosis, this is a serious limitation to the successful application of FR-targeted lipid-based particle delivery systems.

GENE TRANSFECTION *IN VITRO*

The preferential expression of a gene in tumor cells contributes to the safety and efficacy of gene therapy. For FR-targeted gene transfection, the concentrations of folic acid and linker in vectors are important.

Folate Concentration

For drug delivery, FR-targeting liposomes contained 0.1-0.5 mol% folate-PEG-lipid and about 4 mol% PEG-lipid for the PEG-coating were used [8-14]. For gene delivery *in vitro*, a FR-targeting cationic nanoparticle incorporating 2 mol% folate-PEG_{3400}-DPPE showed efficient FR-dependent cellular

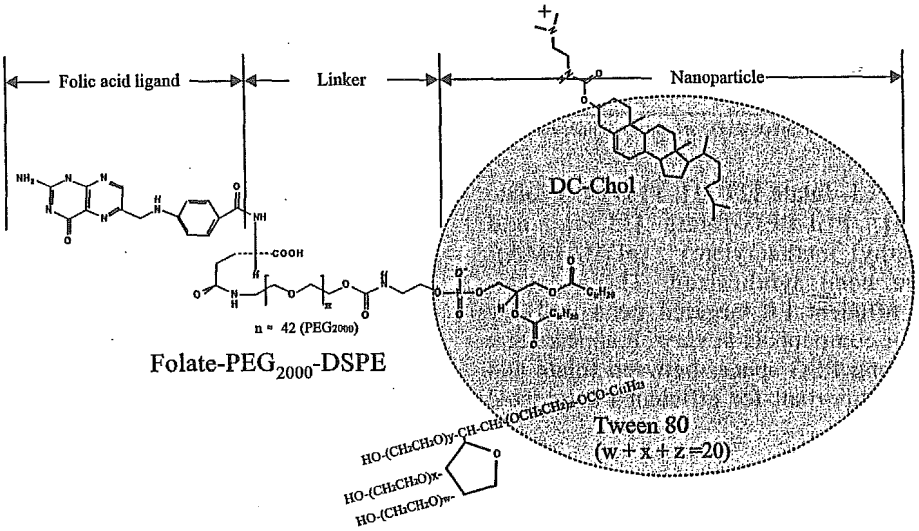

Fig.(2). Schematic structure of the folate-linked nanoparticles composed of folate-PEG_{2000}-DSPE, DC-Chol and Tween 80 (NP-F).

Table 2. Formulae, Particle Size and ζ-Potential of Folate-Linked Nanoparticles and their Nanoplexes [41]

Formulation	Mol (%)			Nanoparticle		Nanoplex[a)]	
	DC-Chol	Tween 80	Folate-PEG_{2000}-DSPE (F)	Size (nm)	ζ-potential (mV)	Size (nm)	ζ-Potential (mV)
NP	95	5	-	117.2 ± 2.0	53.1 ± 2.5	354.9 ± 8.8	39.0 ± 1.0
NP-1F	94	5	1	146.1 ± 12.4	43.9 ± 1.7	515.2 ± 32.3	34.2 ± 1.6
NP-2F (NP-F)	93	5	2	165.3 ± 22.1	38.6 ± 1.5	233.7 ± 6.5	30.8 ± 1.9
NP-3F	92	5	3	118.4 ± 4.3	54.8 ± 6.3	396.0 ± 7.8	35.1 ± 0.9

Nanoparticles were prepared with lipids (e.g. DC-Chol/Tween 80/folate-PEG_{2000}-DSPE=94/5/2, molar ratio = 10:1.3:1.3, weight (mg)) in 10 ml of water by a modified ethanol injection method. Nanoparticles consisted of 1 mg/ml DC-Chol and 5 mol% Tween 80 with 0, 1, 2 and 3 mol% folate-PEG_{2000}-DSPE (NP, NP-1F, NP-2F and NP-3F, respectively). [a)] Charge ratio (+/-) of nanoparticle/DNA = 3/1 Each value represents the mean ± SD (n=3).

uptake and transfection [39], and cationic liposomes with 5 mol% folate-PEG_{4600}-Chol showed high gene transfer activity into a FR-positive cell line, M109 [20]. Reddy *et al.* [21] reported that the liposome formulated with less than 0.03% of folate-PEG_{3400}-DSPE showed the greatest cell association. The folate moieties located at the distal end of the PEG spacers would likely not interact with each other at concentrations lower than 0.03%. Bruckheimer *et al.* [37] reported that 2 mol% of folate-PEG_{3400}-DSPE conjugate increased the cellular association with tumor cells and transfection potency. Xu *et al.* [36] reported specific *in vivo* gene delivery to tumors with a liposome containing about 5 mol% folate-DOPE. Among folate-linked nanoparticles with 1 - 3 mol% folate-PEG_{2000}-DSPE, NP-2F (2 mol%) showed high transfection efficiency in nasopharyngeal cancer KB cells, which overexpressed FR, being comparable to Tfx20, a commercially available DNA transfection reagent (Fig. 3). NP-3F (3 mol%) decreased transfection efficiency. One explanation is that NP-3F might not incorporate 3 mol% of folate-PEG_{2000}-DSPE. A reduction in the ζ-potential with the addition of folate-PEG_{2000}-DSPE was not observed in NP-3F (about 55 mV) (Table 2). Another explanation is that the PEGylated lipid interferes with the intracellular trafficking of complexes, resulting in reduced transgene expression [42]. Therefore, we used NP-2F, containing 2 mol% folate-PEG_{2000}-DSPE, hereafter referred to as NP-F, as a FR-targeting vector.

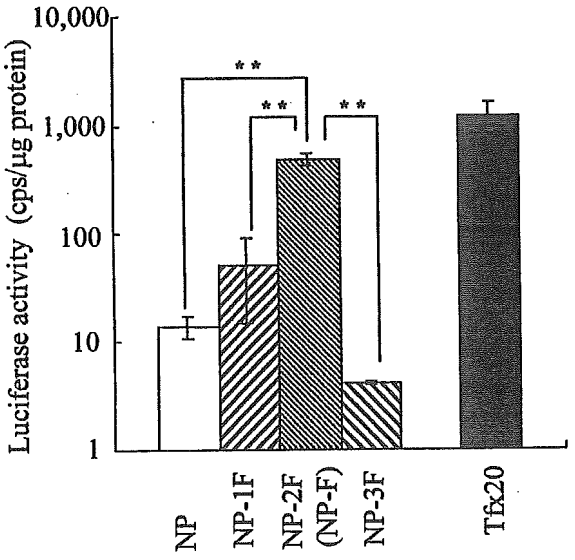

Fig. (3). Comparison of transfection efficiency in KB cells with luciferase expression between nanoparticles and Tfx20. The nanoplex and the lipoplex were prepared by mixing 2 μg of plasmid DNA with the luciferase gene under the control of the cytomegalovirus (CMV) promoter, with nanoparticles and Tfx20, respectively. The luciferase assay was carried out 24 h after the incubation of nanoplexes in medium with 10% serum. Each column represents the mean±S.D. (n=3). $^{**}P<0.01$, compared with NP-F.

Linker

PEG of Mr 2,000 to 5,000 has been used as a linker (Table 1). A certain distance between the folate moiety and the lipid particles is needed for FR-targeting. This is believed to be due to the need for folate to enter the binding pocket of FR on the cell surface. Lee *et al.* [43] were the first to describe the dependence of folate-liposome-targeting on the distance between the folate and liposome, and reported that a PEG_{3400} linker was necessary for the targeting. Leamon *et al.* [17] optimized the targeting activity of the liposomes by modifying the length of the PEG-linker, and found that PEGs as small as Mr 1,000 could function as effective linkers. Ward *et al.* [31] reported that a folate-linked PEG_{800}polymer-modified PLL/DNA complex did not lead to a significant increase in *in vitro* transgene expression. A PEG spacer > Mr 1,000 might be essential for FR-targeting.

Transfection Activity in Various Cells

NP-F showed greater transfection efficiency in human prostate cancer LNCaP cells, human prostate adenocarcinoma PC-3 cells, and human cervix carcinoma Hela cells, than in KB cells, in comparison with Tfx20 (Fig. 4A). There were three FR isoforms, α, β and γ, each with a distinctive tissue distribution [6,24,25]. FR-α mRNA was expressed strongly in KB and Hela cells, but not expressed in LNCaP or PC-3 cells (Fig. 4B). FR-β and -γ mRNAs were not de-

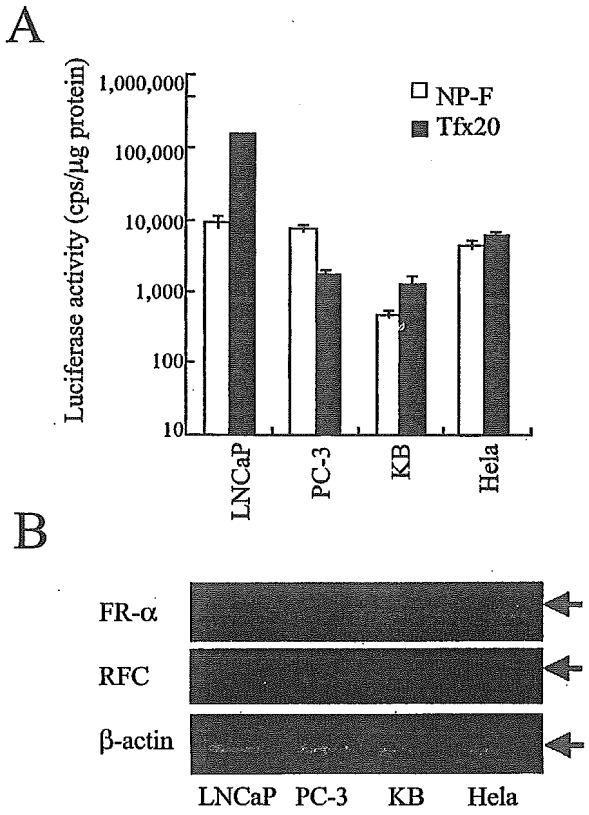

Fig. (4). Comparison of transfection efficiency between NP-F and Tfx20 in the NP-F nanoplexes and Tfx20 lipoplex delivered with the luciferase plasmid into various cell lines (A). Each column represents the mean ± S.D. (n=3). FR-α, RFC and β-actin mRNA expression was detected in various cell lines by RT-PCR (B) [41].

tected in any of the cell lines using the RT-PCR method. Reduced folate carrier (RFC), a carrier-mediated folate transporter, was weakly expressed in all cell lines examined (Fig. 4B). The cellular uptake of NP-F in Hela and KB cells was mediated *via* FR-α, following the induction of transfection activity. The selectivity of NP-F to carry genes into KB cells was examined using FITC-oligodeoxynucleotide (FITC-ODN) by flow cytometry [41]. An association *via* interaction between the folate moiety of NP-F and FR of KB cells was a major route of transfection for the NP-F nanoplex, from the result of competitive experiment in the presence of 1 mM folic acid [41].

In LNCaP and PC-3 cells, FR mRNAs were not often observed. In the human prostate, a high-affinity folate binding protein was characterized [44], and folic acid binds to the membrane fraction that cross-reacts with the anti-prostate-specific membrane antigen (PSMA) antibody. PSMA is a transmembrane protein with a pattern of overexpression restricted to malignant human prostate tissue and LNCaP cells [45]. The physiological role of PSMA in prostate cancer remains unknown, but PSMA shows hydrolase enzymatic activity with a folate substrate [45] and is internalized *via* an endocytic mechanism [46]. If PSMA functions as a receptor mediating the internalization of a putative ligand similar to folic acid, this suggests that the folate-linked nanoparticle binds to PMSA and is then taken up *via* an endocytic mechanism by LNCaP cells as we reported [40]. In PC-3 cells, our study using RT-PCR confirmed the presence of RFC mRNA, but found no FR or PSMA mRNA [41]. An FITC-labeled folate-BSA conjugate was taken up by PC-3 cells and the cellular association was significantly decreased in the presence of 1 mM folic acid [41]. Xu *et al.* [36] also reported that a folate-cationic liposome system could mediate gene therapy with p53 antisense DNA in prostate cancer (DU145 cells). We found that NP-F is a useful vector for transfection in prostate androgen-dependent and independent cancer cells as well as KB cells.

GENE TRANSFECTION *IN VIVO*

Both systemic and local administration offers several biological opportunities for gene therapy. The systemic route allows non-invasive access to many target cells that are not accessible otherwise by direct administration.

Systemic Administration

The folate-linked liposomes showed efficient FR-dependent cellular uptake and transfection *in vitro*. However, the use of a folate ligand as a targeting ligand to deliver DNA has not been successful in *in vivo* gene therapy [20,21]. The major limitation of *in vivo* gene therapy using liposomes is the low transfection efficiency. Several factors have the potential to adversely affect FR-targeted gene transfer *in vivo*. The first is the presence of endogenous folate in the systemic circulation, which potentially can block FR-binding. Plasma folic acid may interfere with the binding of FR. The human serum folic acid concentration, following FDA-mandated dietary supplementation, is ~42 nM [47]. Earlier reports [43] indicated that serum folic acid at this concentration should not significantly inhibit the binding of FR mediated by liposomes. Our recent study [41] showed that the mice were actually able to maintain a plasma folate level within the physiological range of humans on a folate-deficient diet. In contrast, the mice on a normal diet maintained a much higher serum concentration of folic acid. Therefore, mice on a folate-deficient diet should be considered relevant to humans with respect to serum folate levels. A second concern is that the size of gene transfer vectors, escaping the vasculature and intratumoral diffusion, could be limiting to targeted delivery. To address this issue, formulation parameters can potentially be optimized to improve the pharmacokinetic properties of the vectors. For example, the vector can be PEGylated to reduce plasma protein binding and RES uptake, which results in an extended systemic circulation time [48]. In addition, the size of the vector should be kept under 300 nm, since this is the approximate limit for efficient tumor extravasation. Non-specific cell uptake by the RES (for example, Kupffer cells in the liver) is expected to be reduced by incorporating PE-Gylated lipid within the lipid-DNA complex.

When the NP-F nanoplex was injected *via* a tail vein, DNA in the blood was still detectable 4 h later by PCR (Fig. 5). Free DNA is known to have an extremely short $T_{1/2}$ in blood (0.5-1 h) depending on the DNA dose [27,49]. The NP-F seemed to keep the DNA stable in circulation by forming a nanoplex. NP-F induced greater gene expression in liver and kidney than NP (unpublished data). Recently, Paulos *et al.* discovered that activated liver-derived macrophages (Kupffer cells) in mice do express the FR [50]. The Kupffer cells in the liver and apical membrane of the proximal tubes in kidneys of mice may be responsible for capturing NP-F. Therefore, FR-targeted delivery of therapeutic genes damages normal cells in organs such as the liver and kidney and may subsequently cause death. For cancer gene therapy, using a tumor-specific promoter to regulate expression transcriptionally in target cancer cells has promise. It will be essential to use a strong and tissue-specific promoter region if a therapeutic gene is to be selectively expressed in the cancer cells.

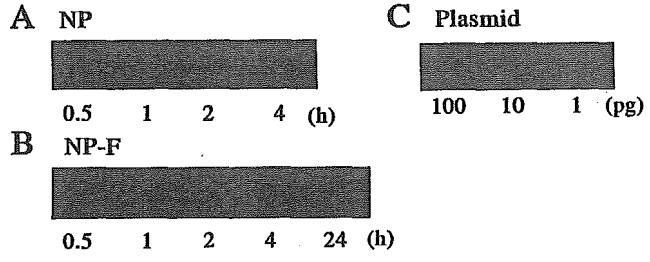

Fig. (5). PCR analysis of plasmid DNA in blood after intravenous administration (A and B). Nanoplexes of 50 μg of plasmid were injected into the tail of male BALB/c mice. At 1, 2, 4 and 24 h after the administration of nanoplexes, blood samples were taken *via* a tail vein, and then DNA was isolated from the blood. DNA samples were diluted with water to a final concentration of 1 ng/ml for PCR analysis. The plasmid DNA was amplified by PCR using 1 ng of DNA from the blood as a template with luciferase-specific primers. PCR products were analyzed by agarose gel electrophoresis. A, NP; B, NP-F; C, control (1, 10, and 100 pg of plasmid as a template for PCR).

Local Administration

Intraperitoneal and intratumoral injections of lipoplex and nanoplex have been applied in mice bearing tumors. Reddy *et al.* [21] reported that maximum *in vivo* transfection activity of reporter gene (luciferase) occurred with intraperitoneally administered folate-liposome using a disseminated intraperitoneal L1210A tumor model. When the NP-F nanoplexes of the luciferase plasmids were injected directly into the nasopharyngeal tumor, KB, xenografts, NP-F showed about 100-fold more luciferase activity than Tfx20, suggesting that the NP-F nanoplex remained small enough to migrate into the tumorous tissue [41].

APPLICATION OF SUICIDE GENE THERAPY

Cancer gene therapy has become an increasingly important strategy for treating a variety of human diseases [1]. Currently, much cancer gene therapy research is being carried out, especially in the field of cancer treatment [51]. Suicide gene therapy is a strategy whereby a gene is introduced into cancer cells, making them sensitive to a drug that is normally non-toxic. The suicide genes used often encode enzymes that metabolize non-toxic prodrugs into toxic metabolites. One of the most frequently used suicide genes is the herpes simplex virus thymidine kinase (HSV-tk) gene [52], which phosphorylates a prodrug, ganciclovir (GCV), into a toxic form (GCV triphosphate, GCV-PPP). GCV-PPP blocks the DNA synthesis machinery and kills the cell. A powerful characteristic of HSV-tk/GCV therapy is that the transduction of a small fraction of tumor cells with the suicide gene can result in widespread tumor-cell death (bystander effect) (Fig. 6). The cell to cell transfer of HSV-tk-activated GCV between HSV-tk-transduced tumor cells and neighboring unmodified cells *via* gap junctions, is a major mechanism of the bystander effect [53,54]. Gap junctions are composed of connexin subunits and connect the cytoplasmic domains of contacting cells, allowing ionic and metabolic exchange between them [55].

The use of a folate ligand as a targeting ligand to deliver DNA has not been successful in *in vivo* gene therapy [20,21]. In prostate cancer, suicide gene therapy by local injection using adenoviral vectors has been reported as an alternative treatment [56,57]. The use of non-viral vectors is a novel approach. An NP-F nanoplex of HSV-tk was transiently transfected into KB, LNCaP and PC-3 cells. The first evidence of transfection was that GCV-PPP, the most abundant triphosphate produced, was clearly detected in LNCaP cells transfected with the HSV-tk gene after incubation with GCV by HPLC (Fig. 7). These findings were also made in KB and PC-3 cancer cells [41]. Further evidence was that HSV-tk plasmid-transfected LNCaP cells showed significantly greater sensitivity to GCV than the controls (IC_{50}; 9.4 μg/ml) (Fig. 8). HSV-tk plasmid-transfected PC-3 cells showed significantly increased sensitivity to GCV compared with the controls (IC_{50}; 66 μg/ml) [41].

The *in vivo* anti-tumor effect of the NP-F nanoplex with the HSV-tk gene was evaluated. When the NP-F nanoplex of the HSV-tk plasmid was injected directly into the tumor, the growth of KB nasopharyngeal tumors was significantly inhibited in the mice treated with the plasmid on day 13 (Fig. 9). A comparison of tumor weight and appearance after excision also demonstrated that the tumor growth was attenuated in the mice treated with the HSV-tk plasmid [41]. The observed reduction in tumor size may not be wholly due to the direct effect of the phosphorylated GCV on the transduced

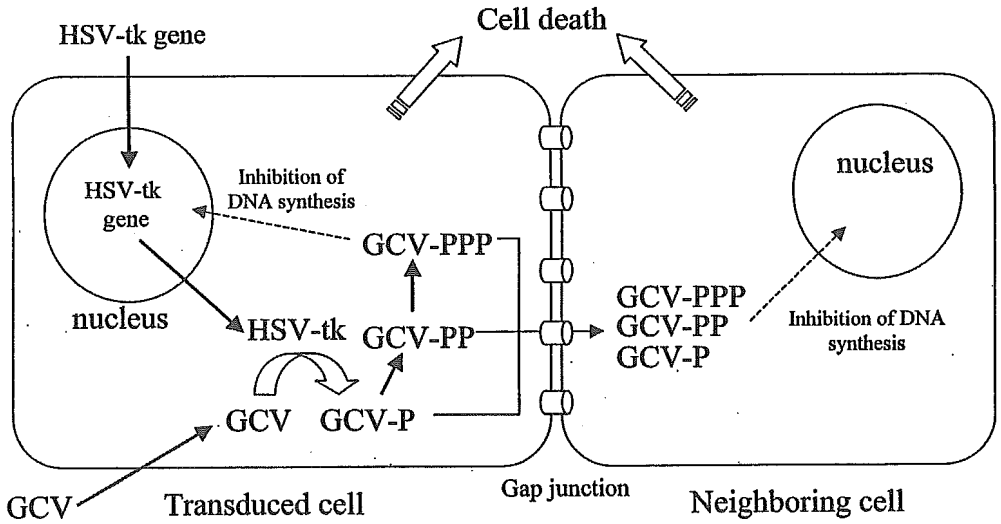

Fig. (6). Schematic representation of the HSV-tk/GCV system's mode of action and the bystander effect. In HSV-tk-transduced cells, GCV is intracellularly phosphorylated and converted to the triphoshate derivative (GCV-PPP), which acts as a competitive inhibitor of deoxyguanosine triphosphate. The production of GCV monophosphate (GCV-P) appears to be catalyzed by HSV-tk in the transduced cells. Subsequent formation of the diphosphate and triphosphate GCV derivatives (GCV-PP and -PPP) is catalyzed by cellular guanylate kinase. After the incorporation of GCV-PPP into DNA, the synthesis of DNA is immediately inhibited in the cells and this leads to cell death. The cell to cell transfer of HSV-tk-activated GCV between HSV-tk-transduced tumor cells and neighboring cells *via* gap junctions is a major mechanism of the widespread tumor-cell death (bystander effect).

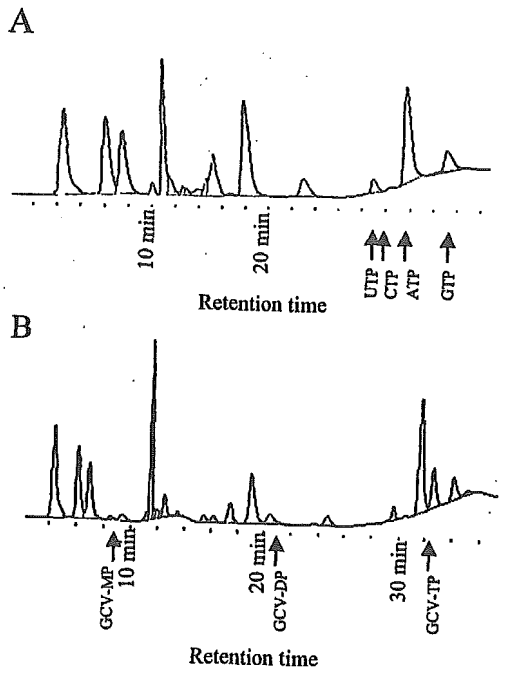

Fig. (7). Anion-exchange HPLC of GCV metabolites in HSV-tk-transfected LNCaP cells using NP-F. The extracts from the non-transfected cells (A) and from the HSV-tk-transfected cells (B) obtained following incubation with 100 μg/ml GCV for 24 h were subjected to HPLC with a gradient of ammonium phosphate (0.02-0.6 M) [41].

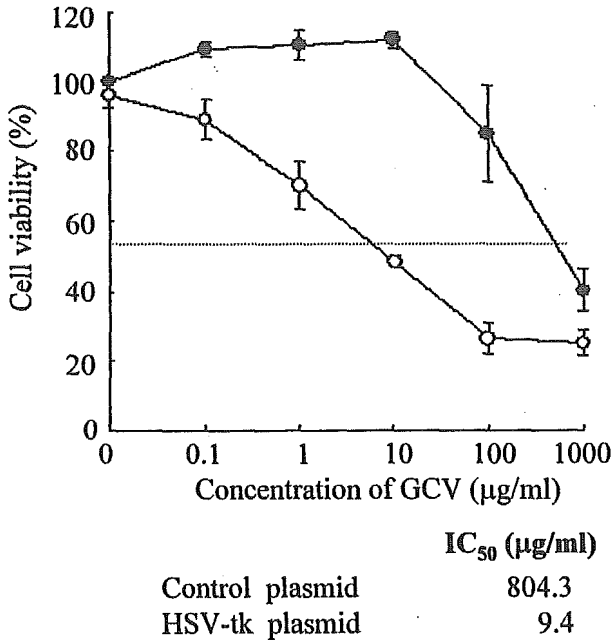

Fig. (8). Sensitivity of LNCaP cells to GCV. The cells were transfected with HSV-tk plasmids using NP-F. After 12 h incubation, the culture medium was replaced with one containing a concentration of GCV ranging form 0.1 to 1,000 μg/ml. The number of surviving cells was determined with a WST-8 assay after 4 days' exposure to the GCV. The plasmids used were: pGL3-enhancer as a control plasmid (●) and HSV-tk (○). Data points indicate the mean±S.D. (n=3).

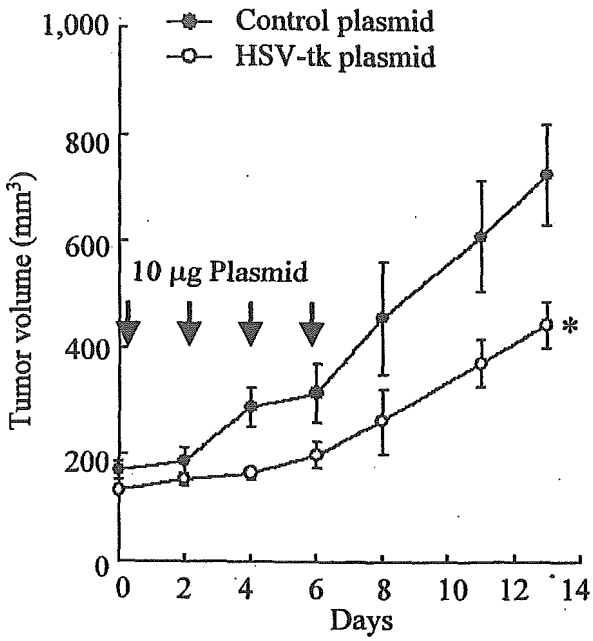

Fig. (9). *In vivo* suicide gene therapy for KB xenografts with GCV in mice. Mice were divided into two groups: group I, noncoding plasmid (10 μg); group II, HSV-tk plasmid (10 μg). The NP-F nanoplexes of the plasmids were injected directly into the KB tumor four times (day 0, 2, 4, and 6). GCV (25 mg/kg) was administered i.p. at 24 and 36 h after the injections. The results indicate the mean volume± S.E. (n=5). *$P<0.05$, compared with the control.

tumor cells. An indirect mechanism (the bystander effect) might be contributing to the anti-tumor activity. It is reported that a 1-5% *in vivo* transfection efficiency could generate a significant anti-tumoral effect in suicide gene therapy [58]. However, a deficiency of gap junctions is found in human prostate tumors [59,60], which may limit the extent of the bystander effect in suicide gene therapy. Therefore, to examine the *in vivo* anti-tumor effect of direct injection into LNCaP prostate xenografts, the nanoplex of HSV-tk plus connexin plasmids was used with the result that the tumor growth was suppressed [41].

CONCLUSION

In this review, we showed that folate-linked, lipid-based nanoparticles could deliver DNA with high transfection efficiency and selectivity, inhibiting tumor growth following intratumoral injection into human nasopharyngeal and prostate cancer using an HSV-tk/GCV therapy system. These findings indicate that folate-linked, lipid-based nanoparticles have potential as a clinically effective vector in cancer suicide gene therapy. However, there is generally little correlation between *in vitro* and *in vivo* gene transfer efficacies of vector formulations, due to very different parameters. For systemic administration, a balance of long-circulating vectors and FR-targeting vectors will be key to using folate-PEG-lipid. Further efforts aimed at optimizing FR-targeting vector formulations for systemic administration should lead to the clinical evaluation of these vectors for cancer gene therapy.

LIST OF ABBREVIATIONS

CHEMS	=	Cholesteryl hemisuccinate
Chol	=	Cholesterol
DC-Chol	=	3([*N*-(*N'*,*N'*–dimethylaminoethane)-carbamoyl] cholesterol
DOPE	=	Dioleoyl phosphatidylethanolamine
DPPE	=	Dipalmitoyl phosphatidylethanolamine
DSPE	=	Distearoyl phosphatidylethanolamine
FR	=	Folate receptor
GCV	=	Ganciclovir
HSV-tk	=	Herpes simplex virus thymidine kinase
PEI	=	Polyethylenimine
PLL	=	Poly-L-lysine
PEG-DSPE	=	Polyethyleneglycol-distearoylphosphatidylethanolamine
PSMA	=	Prostate specific membrane antigen
RES	=	Reticuloendothelial systems
RFC	=	Reduced folate carrier

REFERENCES

[1] Dass,C.R.; Burton, M.A. *J. Pharm. Pharmacol.*, **1999**, *51*, 755-770.
[2] Rosenberg, S.A.; Aebersold, P.; Cornetta, K.; Kasid, A.; Morgan,R. A.; Moen, R.; Karson, E.M.; Lotze, M.T.; Yang, J.C.; Topalian, S.L. *N. Engl. J. Med.*, **1990**, *323*, 570-578.
[3] Hoffman, M. *Science*, **1991**, *252*, 374.
[4] Flotte, T.R.; Solow, R.; Owens, R.A.; Afione, S.; Zeitlin, P.L.; Carter, B.J. *Am. J. Respir. Cell Mol. Biol.*, **1992**, *7*, 349-356.
[5] Dachs, G.U.; Dougherty, G.J.; Stratford, I.J.; Chaplin, D.J. *Oncol. Res.*, **1997**, *9*, 313-325.
[6] Wu, M.; Gunning, W.; Ratnam, M. *Cancer Epidemiol. Biomarkers Prev.*, **1999**, *8*, 775-782.
[7] Antony, A.C. *Annu. Rev. Nutr.*, **1996**, *16*, 501-521.
[8] Lee, R.J.; Low, P.S. *Biochim. Biophys. Acta*, **1995**, *1233*, 134-144.
[9] Gabizon, A.; Horowitz, A.T.; Goren, D.; Tzemach, D.; Mandelbaum-Shavit, F.; Qazen, M.M.; Zalipsky, S. *Bioconjug. Chem.*, **1999**, *10*, 289-298.
[10] Goren, D.; Horowitz, A.T.; Tzemach, D.; Tarshish, M.; Zalipsky, S.; Gabizon, A. *Clin. Cancer Res.*, **2000**, *6*, 1949-1957.
[11] Pan, X.Q.; Zheng, X.; Shi. G.; Wang, H.; Ratnam, M.; Lee, R.J. *Blood*, **2002**, *100*, 594-602.
[12] Pan, X.Q., Wang, H.; Lee, R.J. *Pharm. Res.*, **2003**, *20*, 417-422.
[13] Gabizon, A.; Horowitz, A.T.; Goren, D.; Tzemach, D.; Shmeeda, H.; Zalipsky, S. *Clin. Cancer Res.*, **2003**, *9*, 6551-6559.
[14] Shiokawa, T.; Hattori, Y.; Kawano, K.; Ohguchi, H.; Kawakami, H.; Toma, K.; Maitani, Y. *Clinical Cancer Research*, **2005**, in press.
[15] Reddy, J.A.; Dean, D.; Kennedy, M.D.; Low, P.S. *J. Pharm. Sci.*, **1999**, *88*, 1112-1118.
[16] Lee, R.J.; Huang, L. *J. Biol. Chem.*, **1996**, *271*, 8481-8487.
[17] Leamon, C.P.; Cooper, S.R.; Hardee, G.E. *Bioconjug. Chem.*, **2003**, *14*, 738-747.
[18] Yang, L.; Li, J.; Zhou, W.; Yuan, X.; Li, S. *J. Control Release*, **2004**, *95*, 321-331.
[19] Wang, S.; Lee, R.J.; Cauchon, G.; Gorenstein, D.G.; Low, P.S. *Proc. Natl. Acad. Sci. USA*, **1995**, *92*, 3318-3322.
[20] Hofland, H.E.; Masson, C.; Iginla, S.; Osetinsky, I.; Reddy,J. A.; Leamon, C.P.; Scherman, D.; Bessodes, M.; Wils, P. *Mol. Ther.*, **2002**, *5*, 739-744.
[21] Reddy, J.A.; Abburi, C.; Hofland, H.; Howard, S.J.; Vlahov, I.; Wils, P.; Leamon, C.P. *Gene Ther.*, **2002**, *9*, 1542-1550.
[22] Sabharanjak, S.; Mayor, S. *Adv. Drug Deliv. Rev.*, **2004**, *56*, 1099-1109.
[23] Weitman, S.D.; Lark, R.H.; Coney, L.R.; Fort, D.W.; Frasca, V.; Zurawski, V.R.Jr.; Kamen, B.A. *Cancer Res.*, **1992**, *52*, 3396-3401.
[24] Shen, F.; Ross, J.F.; Wang, X.; Ratnam, M. *Biochemistry*, **1994**, *33*, 1209-1215.
[25] Shen, F.; Wu, M.; Ross, J.F.; Miller, D.; Ratnam, M. *Biochemistry*, **1995**, *34*, 5660-5665.
[26] Allen, T.M.; Hansen, C.; Rutledge, J. *Biochim Biophys. Acta*, **1989**, *981*, 27-35.
[27] Mahato, R.I.; Kawabata, K.; Takakura, Y.; Hashida, M. *J. Drug Target*, **1995**, *3*, 149-157.
[28] Gabizon, A.; Shmeeda, H.; Horowitz, A.T.; Zalipsky, S. *Adv. Drug Deliv. Rev.*, **2004**, *56*, 1177-1192.
[29] Gottschalk, S.; Cristiano, R.J.; Smith, L.C.; Woo, S.L. *Gene Ther.*, **1994**, *1*, 185-191.
[30] Mislick, K.A.; Baldeschwieler, J.D.; Kayyem, J.F.; Meade, T.J. *Bioconjug. Chem.*, **1995**, *6*, 512-515.
[31] Ward, C.M.; Pechar, M.; Oupicky, D.; Ulbrich, K.; Seymour, L.W. *J. Gene Med.*, **2002**, *4*, 536-547..
[32] Leamon, C.P.; Weigl, D.; Hendren, R.W. *Bioconjugate Chem.*, **1999**, *10*, 947-957.
[33] Guo, W; Lee, R.L. *AAPS. PharmSci.*, **1999**, *1*, E19.
[34] Benns, J.M.; Mahato, R.I.; Kim, S.W. *J. Control Release*, **2002**, *79*, 255-269.
[35] van Steenis, J.H.; van Maarseveen, E.M.; Verbaan, F.J.; Verrijk, R.; Crommelin, D.J.; Storm, G.; Hennink, W.E. *J. Control Release*, **2003**, *87*, 167-176.
[36] Xu, L.; Pirollo, K.F.; Chang, E.H. *J. Control Release*, **2001**, *74*, 115-128.
[37] Bruckheimer, E.; Harvie, P.; Orthel, J.; Dutzar, B.; Furstoss, K.; Mebel, E.; Anklesaria, P.; Paul, R. *Cancer Gene Ther.*, **2004**, *11*, 128-134.
[38] Shi, G.; Guo, W.; Stephenson, S.M.; Lee, R.J. *J. Control Release*, **2002**, *80*, 309-319.
[39] Dauty, E.; Remy, J.S.; Zuber, G.; Behr, J.P. *Bioconjug. Chem.*, **2002**, *13*, 831-839.
[40] Hattori, Y.; Maitani, Y. *J. Control Release*, **2004**, *97*, 173-183.
[41] Hattori, Y.; Maitani, Y. *Cancer Gene Ther.*, **2005**, accepted.
[42] Song, L.Y.; Ahkong, Q.F.; Rong, Q.; Wang, Z.; Ansell, S.; Hope, M.J.; Mui, B. *Biochim. Biophys. Acta*, **2002**, *1558*, 1-13.
[43] Lee, R.J.; Low, P.S. *J. Biol. Chem.*, **1994**, *269*, 3198-3204.
[44] Holm J, Hansen SI, Hoier-Madsen M. High-affinity folate binding in human prostate. *Biosci. Rep.*, **1993**, *13*, 99-105.
[45] Pinto, J.T.; Suffoletto, B.P.; Berzin, T.M.; Qiao, C.H.; Lin, S.; Tong, W.P.; May, F.; Mukherjee, B.; Heston, W.D. *Clin. Cancer Res.*, **1996**, *2*, 1445-1451.
[46] Rajasekaran, S.A.; Anilkumar, G.; Oshima, E.; Bowie, J.U.; Liu, H.; Heston, W.; Bander, N.H.; Rajasekaran, A.K. *Mol. Biol. Cell*, **2003**, *14*, 4835-4845.
[47] Lawrence, J.M.; Petitti, D.B.; Watkins, M.; Umekubo, M.A. *Lancet*, **1999**, *354*, 915-916.
[48] Klibanov, A.L.; Maruyama, K.; Beckerleg, A.M.; Torchilin, V.P.; Huang, L. *Biochim. Biophys. Acta*, **1991**, *1062*, 142-148.
[49] Mahato, R.I.; Kawabata, K.; Nomura, T.; Takakura, Y.; Hashida M. *J. Pharm. Sci.*, **1995**, *84*, 1267-1271.
[50] Paulos, C.M.; Turk, M.J.; Breur, G.J.; Low, P.S. *Adv. Drug Deliv. Rev.*, **2004**, *56*, 1205-1217.
[51] El Aneed, A. *J. Control Release*, **2004**, *94*, 1-14.
[52] Fillat, C.; Carrio, M.; Cascante, A.; Sangro, B. *Curr. Gene Ther.*, **2003**, *3*, 13-26.
[53] Hamel, W.; Magnelli, L.; Chiarugi, V.P.; Israel, M.A. *Cancer Res.*, **1996**, *56*, 2697-2702.
[54] Mesnil, M.; Piccoli, C.; Tiraby, G.; Willecke, K.; Yamasaki, H. *Proc. Natl. Acad. Sci. USA*, **1996**, *93*, 1831-1835.
[55] Lampe, P.D.; Lau, A.F. *Arch. Biochem. Biophys.*, **2000**, *384*, 205-215.
[56] Cheon, J.; Kim, H.K.; Moon, D.G.; Yoon, D.K.; Cho, J.H.; Koh, S.K. *BJU. Int.*, **2000**, *85*, 759-766.

[57] Shalev, M.; Miles, B.J.; Thompson, T.C.; Ayala, G.; Butler, E.B. Aguilar-Cordova E.; Kadmon, D. *World J. Urol.*, **2000**, *18*, 125-129.

[58] Huber, B.E.; Austin, E.A.; Richards, C.A.; Davis, S.T.; Good, S.S. *Proc. Natl. Acad. Sci. USA*, **1994**, *91*, 8302-8306.

[59] Tsai, H.; Werber, J.; Davia, M.O.; Edelman, M.; Tanaka, K.E.; Melman, A.; Christ, G.J.; Geliebter, J. *Biochem. Biophys. Res. Commun.*, **1996**, *227*, 64-69.

[60] Habermann, H.; Ray, V.; Habermann, W.; Prins, G.S. *J. Urol.*, **2002**, *167*, 655-660.

Received: December 17, 2004 Accepted: February 17, 2005

Drug Delivery, 12:349–356, 2005
Copyright © Taylor & Francis Inc.
ISSN: 1071-7544 print / 1521-0464 online
DOI: 10.1080/10717540590968215

Taylor & Francis
Taylor & Francis Group

Characteristics and Biodistribution of Soybean Sterylglucoside and Polyethylene Glycol-Modified Cationic Liposomes and Their Complexes with Antisense Oligodeoxynucleotide

Jing Shi, Wen-Wei Yan, and Xian-Rong Qi
Department of Pharmaceutics, School of Pharmaceutical Sciences, Peking University, Beijing, China

Yoshie Maitani and Tsuneji Nagai
Institute of Medicinal Chemistry, Hoshi University, Shinagawa-Ku, Tokyo, Japan

A novel cationic liposome modified with soybean sterylglucoside (SG) and polyethylene glycol-distearoylphosphatidylethanolamine (PEG-DSPE) as a carrier of antisense oligodeoxynucleotide (ODN) for hepatitis B virus (HBV) therapy was constructed. Characteristics of the cationic liposomes modified with SG and PEG (SG/PEG-CL) and their complexes with 15-mer phosphorothioate ODN (SG/PEG-CL-ODN complex) were investigated by incorporation efficiency, morphology, electrophoresis, zeta potentials, and size analysis. Antisense activity of the liposomes and ODN complexes was determined as hepatitis B surface antigen (HBsAg) and hepatitis B e antigen (HBeAg) in $HepG_2$ 2.2.15 cells by ELISA. Their tissue and intrahepatic distribution were evaluated following intravenous injection in mice. The complexes gained high incorporation efficiency and intact vesicular structure with mean size at ~200 nm. The SG/PEG-CL-ODN complexes enhanced the inhibition of both HBsAg and HBeAg expression in the cultured $HepG_2$ 2.2.15 cells relative to free ODN. The uptake of SG/PEG-CL and nonmodified cationic liposomes (CL) was primarily by liver, spleen, and lung. Furthermore, the concentration of SG/PEG-CL was significant higher than that of CL in hepatoctyes at 0.5 hr postinjection. The biodistribution of SG/DSPE-CL-ODN complex compare with free ODN showed that liposomes enhanced the accumulation of ODN in the liver and spleen, while decreasing its blood concentration. SG/PEG-CL–mediated ODN transfer to the liver is an effective gene delivery method for cell-specific targeting, which has a potential for gene therapy of HBV infections. SG and PEG-modified cationic liposomes have proven to be an alternative carrier for hepatocyte-selective drug targeting.

Keywords Antisense Oligodeoxynucleotide, Cationic Liposomes, Hepatocytes, Pegylated, Soybean Sterylglucoside

Hepatitis B virus (HBV) is an infectious agent with about 200 million carriers worldwide. Many patients with HBV infection develop chronic hepatitis, cirrhosisi, and hepatocellular carcinoma. Unfortunately, treatment for chronic infection by HBV is far from satisfactory. The most successful therapeutic agent so far available is interferon-alpha, that shows a 40% response rate for patients after completion of therapy (Dusheiko 1995). Since several viruses have become successful targets of the antisense oligodeoxynucleotide (ODN) approach, this strategy may be promising in targeting HBV infection. Several studies have already shown that ODNs are capable of suppressing HBV *in vitro* (Blum et al. 1991; Wu and Wu 1992) and *in vivo* (Offensperger et al. 1993; Soni et al. 1998). ODNs are synthetic DNA molecules that can inhibit gene expression within cells by their capability to bind a complementary mRNA sequence and prevent translation of mRMA, thus providing potentially powerful therapeutic tools against viral diseases and cancer (Wagner 1994). However, these large polyanionic macromolecules possess several inherent characteristics that restrict their preclinical and clinical utility for the therapy of chronic diseases. These include degradation and inactivation by nucleases in plasma and cells (Akhtar, Kole, and Juliano 1991), poor intracellular delivery (Hope et al. 1998), rapid plasma elimination (Crooke et al. 1996), as well as obvious toxicities.

The inclusion of cationic lipids into the liposome formulations could improve the association with polyanionic nucleic acids and facilitate binding and uptake by cell for the presence of positive surface charge on the particles (Hope et al. 1998). Polyethylene glycol-distearoylphosphatidylethanolamine (PEG-DSPE) is a phospholipid derivative of the hydrophilic polymer polyethylene (Mr = 2,000). Recently it Meyer

Received 30 September 2004; accepted 16 December 2004.
We thank Prof. Lai Wei and his research group at the Institute of Hepatology, Peking University, for assistance in cell culture. This work was supported by the National Natural Science Foundation of China, 30371265.
Address correspondence to Xian-Rong Qi, Department of Pharmaceutics, School of Pharmaceutical Sciences, Peking University, Beijing 100083, China. E-mail: qixr2001@yahoo.com.cn

et al. (1998) found that such derivative of PEG can stabilize the particle of cationic liposome plasmid-DNA complexes *in vitro* and that sterically stabilized liposomes containing PEG-DSPE have long circulation lifetime. Therefore, incorporation of PEG-DSPE into our cationic liposomes would increase particle stability of liposome-ODN complexes and would enhance more targeting by combination of ligand.

Gene transfer to hepatocytes should be of great therapeutic potential since hepatocytes are responsible for the synthesis of a wide variety of proteins, which play important physiological roles in or outside the hepatocytes. Cationic liposomes have been used for hepatic gene transfer to a variety of cell types or for somatic gene therapy. An attempt has been made to transfer the hepatitis C virus (HCV) genome into rat liver with Lipofectin, and the expression of HCV RNA transcripts and HCV core protein has been confirmed (Takehara et al. 1995). Additionally, asialoglycoprotein (AGP)-labeled cationic liposomes have been shown to be highly effective in targeting HepG2 cells through a receptor–mediate gene transfer mechanism, because there are AGP receptors (AGP-R) on hepatocytes and HepG2 cells (Koike et al. 1994).

Soybean sterylglucoside (SG) remains in the residue of soybean after the oil has been extracted. A previous study showed that dipalmitoylphosphatidylcholine (DPPC)-liposome containing SG had a high degree of liver association *in vivo* that might be related to recognition of glucose residues of SG by ASGP-R in hepatocytes. SG in the membrane of cationic liposomes may improve the cell specification of the liposomes and could be helpful for the development of hepatocyte specific ODN-carrier (Shimizu et al. 1998).

In the present study, we constructed a novel liposome carrier of a 15-mer ODN for the HBV therapy. To improve the stability and liver targeting of the cationic-ODN complexes, modification of PEG-DSPE and SG was introduced into the liposome. Their tissue and intrahepatic distribution of the novel liposome were evaluated following intravenous injection in mice.

MATERIALS AND METHODS

Human hepatoma cell line $HepG_2$ 2.2.15 cells were kindly provided by People's Hospital of Peking University (Beijing, China). KM male mice (18–25 g) were obtained from the Institute of Zoology, Chinese Academy of Sciences (Beijing, China). ODN was synthesized with phosphorothioate backbone chemistry by Beijing AUGCT Biological Co. (Beijing, China) and purified by SDS-PAGE, the 5′-3′ sequence of ODN was 5′>GAT GAC TGT CTC TTA <3′, the target site of ODN is the cap site of mRNA transcribed from the SP-II promoter (cap site/SPII). SG was generously supplied by Ryukakusan Co. (Tokyo, Japan). DPPC and PEG-DSPE were purchased from NOF (Tokyo, Japan); 3β-[N-(N′,N′-dimethylaminoethane)-carbamoyl] cholesterol (DC-Chol) was synthesized according to the method described by Gao and Huang (1991). As for radiolabeled liposome, ^{3}H-cholesterol (^{3}H-chol) and ^{125}I-ODN were purchased form China Institute of Atomic Energy (Beijing, China). Collagenase (II) was purchased from Sigma (St. Louis, MO, USA). All other chemicals were of reagent grade.

Preparation of Cationic Liposomes

Multilamellar vesicles were prepared by thin film method. Briefly, the lipids mixture was dissolved in a small volume of chloroform and the organic solvent was slowly removed under reduced pressure on a rotary evaporator for ~2 hr. The thin film was hydrated by adding 1 ml 5% glucose solution (5% Glu) with or without ODN at room temperature by vortex mixture. Then the multilamellar vesicles were sonicated in bath sonicator for 10 min at room temperature and then extruded through 0.2-μm pore sized polycarbonate filters to generate large unilamellar liposomes. The ^{3}H-labeled liposomes included cationic liposomes without modification (CL: DPPC/DC-Chol, 10:10, molar ratio) and SG/PEG-ESPE modified cationic liposomes (SG/PEG-CL: DPPC/DC-Chol/PEG-DSPE/SG, 10: 10:1.34:1.34, molar ratio) were prepared. The radioactivity of liposomes was 4 μCi/200 μl. As for ODN complex, cationic liposomes-ODN complexes without modification (CL-ODN complexes: DC-Chol/ODN, 1:15, molar ratio) and SG/PEG-DSPE-modified cationic liposomes-ODN complex (SG/PEG-CL-ODN complexes: DC-Chol/ODN, 1:15, molar ratio) were prepared, and the amount of ^{125}I-radiolabel was 6 μCi/200 μl.

The incorporation efficiency was determined by equilibrium dialysis. Briefly 1 ml of ODN cationic liposomes complexes (ODN at 0.33 μg) was taken separately in a dialysis tubing (SpectraPor 12,000 to 14,000 mwco) and placed in 10 ml of 5% Glu and incubated at 0°C for 12 hr. The outer phase was taken and the concentration of ODN was detected by ultraviolet spectrophotometer at 260 nm.

Liposomes size and zeta potentials in 5% Glu were determined using a Zetasizer 3000HS (Malvern Instruments, Ltd., UK). The morphology of liposomes and complex also was researched by the Hitachi-500 transmission electron microscope (Hitachi, Japan).

Electrophoresis

First, 450 mg Agarose (Sigma) was dissolved in 150 ml of electrode buffer (pH adjusted to 8.0) and cast as a 2.5-mm thick slab using a Horizon 58 (Bethesda Research Laboratories, Life Technologies) apparatus. Electrophoresis was at 100 V for 10 min. Then, the gel was graphed by an AmpGene UV 3000 gel image system (Yongding Technical Development Co. Ltd).

Samples tested in the electrohporesis analysis included SG/PEG-CL-ODN complexes, SG/PEG-CL-ODN complexes destructed by Triton X-100, and SG/PEG-CL-ODN complexes incubated with 50% (v/v) rat plasma for 2 hr, respectively. Next, 10 μl containing 0.6 μg of ODN in each sample were analyzed.

Antisense Activity of Cationic Liposomes-ODN Complexes

$HepG_2$ 2.2.15 was culture in DMEM containing 10% FBS at 37°C and 5% CO_2. For lipofection, suspension cells were seeded at an initial concentration of 1×10^4 per well for 96-well plates. When adherent cells reached ~80% confluence, the cells were washed extensively to remove the previously produced HBsAg and HBeAg from the medium. After washing, 100 μl ODN or SG/PEG-CL-ODN complexes at the ODN concentration of 1.25, 2.5, or 5.0 μM with 100 μl DMEM containing 10% serum were added. After washing, 100 μl SG/PEG-CL-ODN complex along with 100 μl DMEM containing 10% serum were added. Culture supernatants were collected at 24, 48, and 72 hr, separately, and at each time the cells were washed and ODN or SG/PEG-CL-ODN complexes and DMEM were added again. Culture supernatants were collected at 24, 48, and 72 hr, separately, each time the cells were washed and new complexes and DMEM were added. The concentration of HBsAg and HBeAg in the culture supernatants was determined by ELASA, following the manual provided by manufacturers.

Biodistribution of ^{3}H-Labeled Cationic Liposomes

The ^{3}H-chol-labeled CL and SG/PEG-CL were injected (4.2 μg DC-Chol per 200 μl) into male mice (18–24 g) via the tail vein at a dose of 4 μCi/20 g body weight. At adequate time periods after injection, mice were sacrificed and the blood was collected. The heart, liver, spleen, kidney, and lung were excised and weighed. Next, 100 μl blood and 50–100 mg tissue samples were taken and decolored by 200 μl $HClO_4$ and 300 μl 60% H_2O_2, finally measured in a Pharmacia-Wallac 1410 liquid scintillation analyzer (Turku, Finland).

Hepatic Cell Distribution of ^{3}H-Labeled Cationic Liposomes

Mice were injected intravenously with ^{3}H-labeled CL and ^{3}H-labeled SG/PEG-CL, respectively, at 4 μCi/20 g body weight. At 0.5 and 4 hr after administration, the mice were anesthetized. After perfused by 0.9% NaCl to remove blood through vena cava, the liver was excised and cut into small pieces in ~1 mm^3. Then the liver was incubated with 0.05% (w/v) collagenase for 30 min. The dispersed cells were filtered through cotton mesh sieves, followed by centrifugation at 500 rpm for 3 min; the pellets containing hepatocytes cells were washed three times with isotonic PBS (pH 7.4) by centrifuging at 500 rpm for 3 min. The supernatant containing nonhepatocytes cells was similarly centrifuged and washed three times at 1500 rpm for 5 min. Then, 100 μl hepatocytes and nonhepatocytes cells were taken, treated, and determined the same way as the organ samples.

Biodistribution of ^{125}I-Labeled Cationic Liposomes-ODN Complexes

The ODN solution and SG/PEG-CL-ODN complexes labeled with trace amounts of ^{125}I-ODN (2.5 μg ODN in 200 μl; molar ratio of cationic lipid and ODN was 15:1) were injected into male mice (18–24 g) via the tail vein at 6 μCi/20 g body weight. At adequate time periods after injection, mice were sacrificed and 100 μl blood were collected. The heart, liver, spleen, kidney, and lung were excised and weighed. Then the samples were counted directly by SN-605B γ-counter (Shanghai, China). The total area under the curve (AUC) from time 0 to infinity was estimated from the sum of successive trapezoids between each data point, plus an estimation of the tail area from the last concentration-time point to infinity.

RESULTS

Characteristics of SG/PEG-CL and its ODN Complexes

Characteristics of these liposomes and liposomes-ODN complexes are shown in Table 1. The complexes yielded high incorporation efficiency when the charge ratio of anionic ODN/cationic lipid was 1:1 (1:15 in molar ratio). The incorporation efficiency of CL-ODN complexes was approximately 91.1%, whereas the encapsulation efficiency of SG/PEG-CL slightly decreased to 89.5%. CL and SG/PEG-CL consisted of homogeneous populations of vesicles with mean size in ~131.3 nm and 132.4 nm, respectively. After corporation of liposomes with ODN, the average size of CL-ODN complexes increased sharply to 436.4 nm, while the size of SG/PEG-CL–ODN complex increased slightly to 197.5 nm. Compared with the cationic liposoems composed of only DC-Chol and DPPC (CL), addition of SG and PEG-DSPE (SG/PEG-CL) increased the positive zeta potential of cationic liposomes from 47.0 mV to 59.6 mV. As for ODN cationic liposomes, the loading of ODN eventually changed the zeta potential to almost neutral values; the zeta potential of SG/PEG-CL-ODN complexes was −3.3 mV, when the ODN /DC-Chol was 1:1 in charge ratio.

TABLE 1
Characteristic of cationic liposomes and their ODN complexes

	Incorporation efficiency[a] (%)	Mean diameter[b] (nm)	Polydispersity[b]	Zeta potential[b] (mV)
CL	—	131.3	0.54	47.0
CL-ODN	91.1 ± 5.1	436.4	1.00	ND[c]
SG/PEG-CL	—	132.4	0.76	59.6
SG/PEG-CL-ODN	89.5 ± 1.2	197.5	0.35	−3.3

CL-cationic liposome without modification; CL-ODN-CL complexd with ODN, the charge ratio of cationic lipid/ODN = 1:1; SG/PEG-CL-SG- and PEG-DSPE-modified cationic liposomes; SG/PEG-CL-ODN-SG/PEG-CL complexd with ODN, the charge ratio of cationic lipid/ODN = 1:1.

[a]The values represent mean ± SD, $n = 3$.

[b]The particle size and zeta potential represent the mean of 2 independent experiments.

[c]Not Determined.

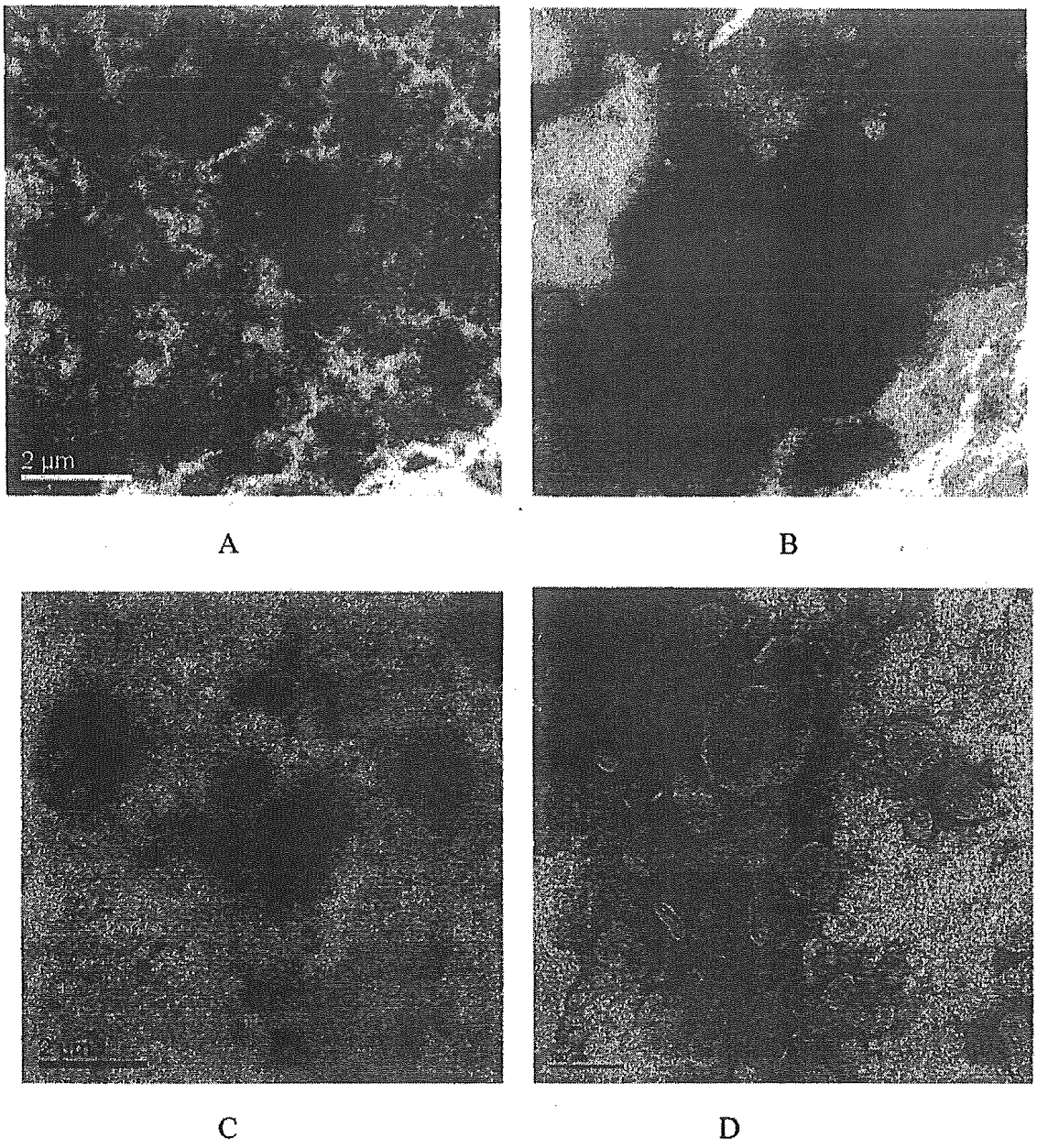

FIG. 1. Transmission electron microscopy of cationic liposomes and their oligonucleotides complexes. (A) Cationic liposomes without modification (CL); (B) SG/PEG-DSPE-modified liposomes (SG/PEG-CL); (C) complexes of nonmodified cationic liposomes with ODN (CL-ODN complexes); (D) complexes of SG- and PEG-DSPE-modified cationic liposomes with ODN (SG/PEG-CL-ODN complexes).

Transmission electron micrographs of CL and SG/PEG-CL showed spherical vesicles, as shown in Figure 1. The presence of SG/PEG-DSPE had little affect on the structure and size of blank cationic liposomes. Vesicle structure and size were greatly influenced by the loading of ODN. As for CL-ODN, no spherical vesicles were observed, the presence of ODN seemed to transform small liposomes into large membrane shape. The addition of SG/PEG-DSPE reserved the spherical shape of liposome-ODN complexes, although aggregation of some of the vesicles also can be observed. The size distribution of complexes seen on electron micrographs corresponded to the values of particle size obtained by dynamic light scattering analysis. Furthermore, in blank cationic lipsomes, the boundaries of the vesicles were smooth, continuous, and intact, whereas when ODN was loaded, the boundaries were often dotted and discontinuous. Thus, the interacting ODN seemed to distort the normally smooth boundaries of the vesicle and caused aggregation of the complexes.

Electrophoresis Analysis

To determine the integrality of SG/PEG-CL-ODN complexes, electrophoresis analysis in used. The result of agarose

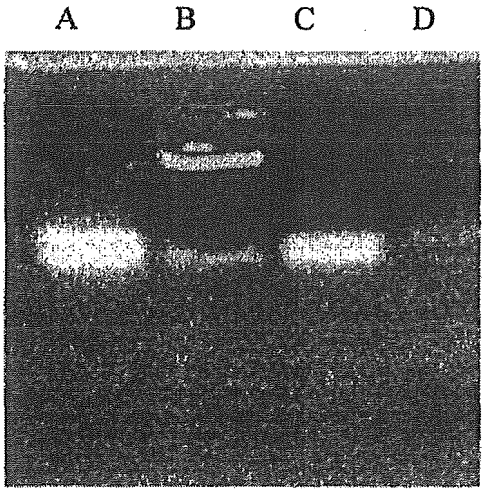

FIG. 2. Agarose gel electrophoresis of SG/PEG-CL-ODN complexes. Fully 10 μl containing 0.6 μg ODN of each sample were analyzed. (A) ODN control; (B) SG/PEG-CL-ODN complexes; (C) SG/PEG-CL-ODN complexes destructed by Triton X-100; (D) SG/PEG-CL-ODN complexes incubated with 50% (v/v) rats plasma for 2 hr.

electrophoresis is shown in Figure 2. Compared with control (only ODN) in the first line, SG/PEG-CL-ODN complexes showed two blots, one faint blot had the same site as control, and the other was bright and still in the initial place. In the third line, the destructed complexes showed only one blot in the control level. This result demonstrated that a part of ODN interacted with cationic liposomes and formed the system in neutral charge, which could not move in the electric field. However, no ODN blot was observed after incubating the complexes with plasma (line D), and such result may relate to the interaction of complexes with plasma components.

Effect of SG/PEG-CL-ODN Complexes on HepG$_2$ 2.2.15 Expression

Figure 3 shows the effect of cellular treatment with free ODN and SG/PEG-CL-ODN complexes on the level of expression of HBsAg and HBeAg protein in HepG$_2$ 2.2.15 cells. The percent of inhibition by ODN varied depending on the concentration of the ODN in the culture medium, especially for the SG/PEG-CL-ODN complexes. When concentration of ODN added in the medium increased from 1.25 μM to 5.0 μM, the inhibition percent of HBsAg by SG/PEG-CL-ODN complexes increased from 59.15% to 90.37% at 72 hr, whereas the inhibition of HBeAg increased from 42.9% to 73.43%. As for inhibition of HBsAg, the effect of free ODN and SG/PEG-CL-ODN complexes was almost the same at 24 hr after incubation, but showed significant difference in the following two time points with the decrease of inhibition effect by free ODN and the increase of inhibition effect by SG/PEG-CL-ODN complexes. The HBeAg inhibition expression showed different tendencies compared with the HBsAg; the inhibition effect of free ODN was overcome by SG/PEG-CL-ODN complexes only when incubation time reached 72 hr.

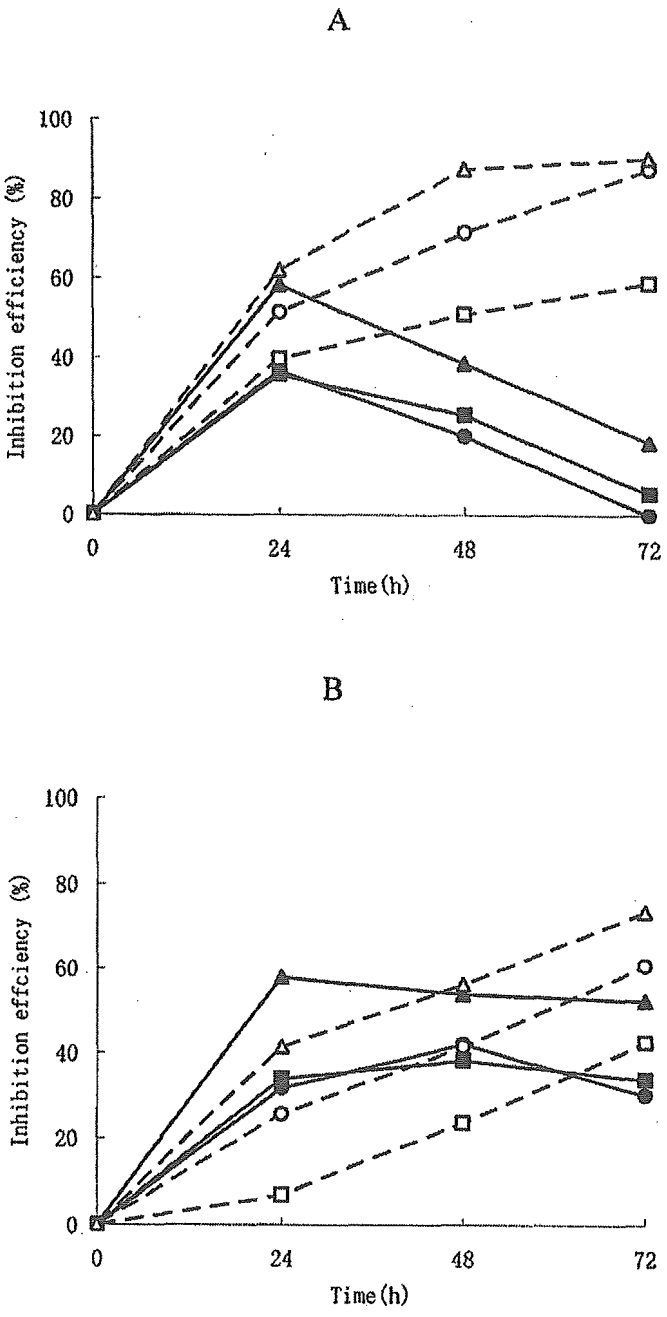

FIG. 3. Effect of SG/PEG-CL-ODN complexes on HBsAg (A) and HBeAg (B) concentration in culture medium. HepG$_2$ 2.2.15 cells were incubated at 37°C in medium containing ODN solution (the continuous line and the solid symbols) or SG/PEG-CL-ODN complexes (the dotted line and the empty symbols). The ODN concentration was 1.25 μM (square), 2.5 μM (round), and 5.0 μM (triangle), respectively.

Biodistribution of ^{3}H-Labeled Cationic Liposomes

The area under the curve (AUC) of the two preparations in different tissues after intravenous injection is shown in Table 2. No significant different in radioactivity was observed at all time points. The injected CL and SG/PEG-CL accumulated primarily in the liver (~70% of the injected dose). Accumulation in the

TABLE 2
$AUC_{0-\infty}$ values of different tissues of the ^{3}H-labeled cationic liposomes after intravenous injection in mice at 4 μCi/20 g body weight

	Blood	Liver	Spleen	Lung	Kidney	Heart
CL	3.90 ± 0.14	5.92 ± 0.66	1.18 ± 0.13	0.92 ± 0.10	0.79 ± 0.10	0.23 ± 0.03
SG/PEG-CL	3.79 ± 0.35	6.95 ± 0.05	1.14 ± 0.05	0.88 ± 0.06	0.68 ± 0.07	0.21 ± 0.01

CL-cationic liposome without modification; SG/PEG-CL-SG- and PEG-DSPE-modified cationic liposomes.
Data represent mean ± SD, $n = 3$.

spleen (~15% or 9% of the injected dose of CL and SG/PEG-CL, respectively) and in the lung (~9% or 7% of the injected dose of CL and SG/PEG-CL, respectively) also was observed. About 2% or less of the injected dose accumulated in the heart and kidney. Thus, the majority of the injected lipid accumulated in the liver. The uptake of injected cationic liposomes by the liver was quite rapid. By 10 min postinjection, ~70% of the injected dose had accumulated in the liver, while only ~14%–18% of the injected dose remained in the circulation. No significant difference between two preparations was observed.

Intrahepatic Cell Distribution of ^{3}H-Labeled Cationic Liposomes

Hepatocytes and nonhepatocytes were separated by infusion method to determine the radioactivity amount in hepatocytes and nonhepatocytes, respectively, as shown in Table 3. The radioactivity of SG/PEG-CL was significantly higher than that of CL in hepatocytes at 0.5 h postinjection ($p < 0.01$), whereas the radioactivity of SG/PEG-CL was significantly lower than that of CL in nonhepatocytes at both 0.5 and 4 hr after intravenous injection ($p < 0.01$).

Biodistribution of ^{125}I-Labeled Cationic Liposomes-ODN Complexes

The biodistribution of the SG/PEG-CL-ODN complexes, labeled with trace amount of ^{125}I-ODN, was determined by intravenous injection, compared with the ODN solution. Rapid clearance was observed in both SG/PEG-CL-ODN complexes and ODN solution. The AUC of the two preparations in different tissues is shown in Table 4. The AUC of SG/PEG-CL-ODN complexes in the liver and spleen were significantly higher than that of ODN solution ($p < 0.01$), meanwhile the AUC in the blood was significantly lower than ODN solution ($p < 0.01$), which may be attributed to the different fate of liposomal particle *in vivo*.

DISCUSSION

It is relatively straightforward to passively encapsulate anionic ODN in the aqueous space of conventional lipid vesicles. However, to achieve even modest incorporation efficiencies of 5–10% in a population of large unilamellar vesicles, extreme concentrations of lipid and ODN must be employed. The inclusion of certain amounts of cationic lipid improves the association of anionic ODN with the vesicles through electrostatic interactions. Entrapment of ODN to cationic liposomes was very efficient even when containing relatively high amounts of SG and PEG-DSPE (6.7 mol %) in the present study. Evidently, PEG coating seldom shields the positively charged liposome surface from interaction with ODN.

The introduction of PEG-DSPE is meant to improve the physical stability of cationic liposomes after complexed with ODN. It was reported that PEG modification could increase the stability of cationic liposome-ODN complexes against aggregation (Remy et al. 1995), and the stabilizing effect of PEG coating on the cationic liposome-ODN complexes is likely to result from preventing cross-linking of vesicles by ODN (Woodle et al. 1992).

TABLE 3
Radioactivity (dpm) distribution of ^{3}H-labeled cationic liposomes in hepatocytes and nonhepatocytes after intravenous injection in mice at 4 μCi/20 g body weight

Time (hr)	Hepatocytes		Nonhepatocytes	
	CL	SG/PEG-CL	CL	SG/PEG-CL
0.5	2068.4 ± 169.9	3488.3 ± 511.5*	1863.4 ± 285.6	1197.4 ± 167.8**
4	926.4 ± 210.7	1141.4 ± 315.8	1035.4 ± 115.1	653.7 ± 5.2***

*$p < 0.01$ vs. CL in hepatocytes at 0.5 hr; **$p < 0.01$ vs. CL in nonhepatocytes at 0.5 hr; ***$p < 0.01$ vs. CL in nonhepatocytes at 4 hr.
CL-cationic liposome without modification; SG/PEG-CL: SG- and PEG-DSPE-modified cationic liposomes.
Data represent mean ± SD, $n = 3$.

TABLE 4
$AUC_{0-\infty}$ values of different tissues of the ^{125}I-labeled ODN solution and SG/PEG-CL-OND complexes after intravenous injection in mice at 6 μCi/20 g body weight

	Blood	Liver	Spleen	Lung	Kidney	Heart
ODN	$1.49 \pm 0.06^{**}$	$0.53 \pm 0.03^{**}$	$0.08 \pm 0.01^{**}$	0.14 ± 0.02	0.30 ± 0.10	0.03 ± 0.00
SG/PEG-CL-OND	0.89 ± 0.25	0.88 ± 0.05	0.27 ± 0.01	0.12 ± 0.02	0.23 ± 0.06	0.02 ± 0.00

SG/PEG-CL-ODN-SG/PEG-CL complexd with ODN, the charge ratio of cationic lipid/ODN = 1:1.
$^{**}p < 0.01$ vs. SG/PEG-CL-OND.
Data represent mean ± SD, $n = 3$.

In our study, PEG-DPSE actually improved the stability of liposome-ODN according to characteristic results. Modification of PEG and SG significantly reduced the particle size of complexes while the spherical vesicle had been investigated in the SG-PEG-CL-ODN complexes instead of the large membrane morphology of CL-ODN complexes (Table 1 and Figure 1). However, aggregation of SG/PEG-CL-ODN complexes also was observed in our study when viewed by transmission electron micrographs. Meanwhile, we also observed that both the CL-ODN complexes and SG/PEG-CL-ODN complexes would form white precipitation after being reserved over a week (data not shown). Therefore, we postulated that although a certain amount of PEG chain had some steric effect on the interaction of vesicles, it could not completely conceal such action, PEG may have a contrary effect when used in the cationic liposomes as others reported: the polymer depletion effect of PEG chain at low concentration (2–5% mol) induce liposomes aggregation (Kuhl et al. 1996).

Addition of ODN sharply modified the zeta potential of SG/PEG-CL-ODN complexes to a value of −3.3 mV, an approximate neutral charge value corresponding to the charge ratio of ODN/cationic lipid in our formulation. The change of zeta potential may result in the loss of stability of the complexes compared with the blank liposmes (SG/PEG-CL) because of the disappearance of static electric repulsion, and these changes may further influence the *in vivo* properties of cationic liposomes and their ODN complexes.

A previous study showed that such ODN could inhibit the expression of HBsAg without significant effect on total synthesized protein in the cells (Wu and Wu 1992). According to the results of our study, the initial concentration of ODN and incubation time appeared to be important factors in obtaining the optimum inhibition effect. With the increase of ODN concentration and incubation time, the inhibition efficiency of SG/PEG-CL-ODN complexes also increased. However, a larger amount of ODN and cationic lipid would lead to higher toxicity to the cells, therefore concentration of cationic liposome-ODN complexes should be restricted in a certain level (Cao and Huang 1991). As for the present SG/PEG-CL-ODN complex, the concentration of DC-Chol lower than 10 μg/ml with cationic lipid/ODN at 1:1 in charge ratio was suitable (data not shown).

In the study of biodistribution of ^{3}H-labeled cationic liposomes, almost no difference was found between the *in vivo* fate of CL and SG/PEG-CL. These results indicate that the PEG chain and glucose residue in SG did not necessarily improve the *in vivo* behavior of cationic lipid. Therefore, we estimated that the cationic charge on the surface of cationic liposomes may be a key factor in their pharmacokinetics and biodistribution. Some investigators have shown that the *in vivo* behavior of cationic liposomes is mainly decided by their zeta potential or the amount of cationic lipid contained in the formulation. Aoki et al. (1997) showed that when the cationic liposomes containd only 5 mol% of charge lipid with small zeta potential, the behavior of the cationic liposomes would not be different from that of neutral liposomes (Zalipsky et al. 1994). Liposomes containing 10 mol% cationic lipid or bearing a zeta potential of ~ +15 mV would remain in blood longer and accumulated less in liver (Aoki et al, 1997; Abraham, Goundalkar, and Mezei 1984). Cationic liposomes containing ~50% of charged lipid were reported to accumulate in the liver rapidly after intravenous injection, and the corresponding zeta potential may be 25 mV or above (Litzinger et al. 1996). These findings agree with ours.

However, in the present study, with almost the same amount of radioactivity detected in the total liver between CL and SG/PEG-CL, hepatocytes targeting of SG/PEG-CL was demonstrated. These results could be attributed to the special behavior of SG to target the hepatocytes. Previous study showed that the glucose residue in SG on the surface of liposomes could be selectively recognized by hepatocytes cells (Shimizu et al. 1997). The result also demonstrated that the hepatocyte targeting effect of SG has not been hindered thoroughly by the PEG chain and positive charge on the surface of liposomes.

The ^{125}I-labeled ODN solution and SG/PEG-CL-ODN complexes showed different *in vivo* behavior compared with SG/PEG-CL. The entrapment of cationic liposome had only a little effect on the biodistribution of ODN. One of the most important factors that may cause such a result is the interaction of SG/PEG-CL-ODN complexes and plasma or serum component. The interaction between cationic liposomes complexes and blood component has always been an obstacle in the application of cationic liposome gene delivery system *in vivo* (Zelphati and Szoka 1996). Zelphati et al.(1998) demonstrated that there were two explanations for serum component inhibition: coating of the complexes with serum components and dissociation of the complex by serum component. Such

interactions also may exist when the complexes are incubated with plasma.

Meyer et al. (1998) reported that after mixing ODN with liposome composed of dioleoylphosphatidylethanolamine, polyethylene glycol-phosphatidylethanolamine, and a cationic lipid, although good incorporation was achieved, ~40% of ODN dissociation occurred upon intravenous injection. A pharmacokinetic experiment indicated that even more dissociation occurred upon intravenous injection (Stuart and Allen 2000). We found in electrophoresis analysis that no blot of ODN was observed after incubating the SG/PEG-CL-ODN complexes with 50% plasma; this may be due to the interaction of plasma component with complexes. The biodistribution result in our study also coincided with these explanations. After the complexes were administered via tail vain, the complexes quickly dissociate in blood. Therefore, the *in vivo* behavior of the complexes was similar to free ODN. However, a portion of ODN was still entrapped in the cationic liposomes, so liver accumulation was observed.

From these studies we propose that interaction with blood components presents a major hurdle for efficient ODN delivery by cationic liposome *in vivo*. However, we also found that SG and PEG-modified cationic liposome is an effective gene delivery method for hepatocyte targeting, which appears to have a potential for gene therapy of HBV infections. Significant progress has been made in recent years in bringing ODN into the clinical setting. By reducing the interaction of plasma components with the injected complex, these barriers to ODN/DNA delivery via cationic liposomes may be overcome.

REFERENCES

Abraham, I., Goundalkar, A., and Mezei, M. 1984. Effect of liposomal surface charge on the pharmacokinetics of an encapsulated model compound. *Biopharm. Drug Dispos.* 5:387–398.

Akhtar, S., Kole, R., and Juliano, R. L. 1991. Stability of antisense DNA oligodeoxynucleotide analogs in cellular extracts and sera. *Life Sci.* 49:169–174.

Aoki, H., Tottori, T., Sakurai, F., Fuji, K., and Miyajima, K. 1997. Effects of positive charge density on the liposomal surface on disposition kinetics of liposomes in rats. *Int. J. Pharm.* 156:163–174.

Blum, H. E., Galun, E., Weizsacker, F., and Wands, J. R. 1991. Inhibition of hepatitis B virus by antisense oligodeoxynucleotides. *Lancet* 337: 1230.

Crooke, S. T., Graham, M. J., Zuckerman, J. E., Brooks, D., Conklin, B. S., Cummins, L. L., Greig, M. J., Guinosso, C. J., Kornbrust, D., Manoharan, M., Sasmor, H. M., Schleich, T., Tivel, K. L., and Griffey, R. H. 1996. Pharmacokinetic properties of several novel oligonucleotide analogs in mice. *J. Pharmacol. Exp. Ther.* 277:923–937.

Dusheiko, G. M. 1995. Treatment and prevention of chronic viral hepatitis. *Pharmacol. Therapeut.* 65:47–73.

Gao, X., and Hang, L. 1991. A novel cationic liposome reagent for efficient transfection of mammalian cells. *Biochem. Biophys. Res. Commun.* 179:280–285.

Hope, M. J., Mui, B., Ansell, S., and Ahkong, Q. F. 1998. Cationic lipids, phosphatidylethanolamine and the intracellular delivery of polymeric, nucleic acid-based drugs. *Mol. Membr. Biol.* 15:1–14.

Koike, K., Hara, T., Aramak, Y., Takada, S., and Tsuchiya, S. 1994. Receptor-mediated gene transfer into hepatic cells using asialoglycoprotein-labeled liposomes. *Ann. NY Acad. Sci.* 716:331–333.

Kuhl, T., Guo, Y., Alderfer, J. L., Berman, A. D., Leckband, D., Israelachvili, J., and Hui, S. W. 1996. Direct measurement of polyethylene glycol induced depletion attraction between lipid bilayers. *Langmuir* 12:3003–3014.

Litzinger, D. C., Brown, J. M., Wala, I., Kaufman, S. A., Van, G. Y., Farrell, C. L., and Collins, D. 1996. Fate of cationic liposomes and their complex with oligonucleotide in vivo. *Biochim. Biophys. Acta* 1281:139–149.

Meyer, O., Kirpotin, D., Hong, K., Sternberg, B., Park, J. W., Woodle, M. C., and Papahadjopoulos, D. 1998. Cationic liposomes coated with polyethlene glycol as carriers for oligonucleotides. *J. Biol. Chem.* 273:15621–15627.

Offensperger, W. B., Offensperger, S., Walter, E., Teubner, K., Lgloi, G., Blum, H. E., and Gerok, W. 1993. In vivo inhibition of duck hepatitis B virus replication and gene expression by phosphorothioate modified antisense oligodeoxynucleotides. *EMBO J.* 12:1257–1262.

Remy, J. S., Kichler, A., Mordvinov, V., Schuber, F., and Behr, J. P. 1995. Targeted gene transfer into hepatoma cells with lipopolyaminecondensed DNA particles presenting galactose ligands: a stage toward artificial viruses. *Proc. Natl. Acad Sci. USA* 92:1744–1748.

Soni, P. N., Brown, D., Saffie, R., Savage, K., Moore, D., Gregoriadis, G., and Dusheiko, G. M. 1998. Biodistribution, stability, and antiviral efficacy of liposome-entrapped phosphorothioate antisense oligodeoxynucleotides in ducks for the treatment of chronic duck hepatitis B virus infection. *Hepatology* 28:1402–1410.

Shimizu, K., Maitani, Y., Takahashi, N., Takayama, K., and Nagai, T. 1998. Association of liposomes containing a soybean-derived sterylglucoside mixture with rat primary cultured hepatocytes. *Biol. Pharm. Bull.* 21:818–822.

Shimizu, K., Maitani, Y., Takayama, K., and Nagai, T. 1997. Formulation of liposomes with a soybean-derived sterylglucoside mixture and cholesterol for liver targeting. *Biol. Pharm. Bull.* 29:81–886.

Stuart, D. D., and Allen, T. M. 2000. A new liposomal formulation for antisense oligodeoxynucleotides with small size, high incorporation efficiency and good stability. *Biochim. Biophys. Acta* 1463:219–229.

Takehara, T., Hayashi, N., Miyamoto, Y., Yamamoto, M., Mita, E., Fusamoto, H., and Kamada, T. 1995. Expression of the hepatitis C virus genome in rat liver after cationic liposome-mediated in vivo gene transfer. *Hepatology.* 21:746–751.

Wagner, R. W. 1994. Gene inhibition using antisense oligodeoxynucleotides. *Nature* 372:333–335.

Woodle, M. C., Collins, L. R., Sponsler, E., Kossovsky, N., Papahaduopoulos, D., and Martin, F. J. 1992. Sterically stabilized liposomes: reduction in electrophoretic mobility but not electrostatic surface potential. *Biohpys. J.* 61:902–910.

Wu, G. Y., and Wu, C. H. 1992. Specific inhibition of hepatitis B viral gene expression in vitro by targeted antisense oligonucleotides. *J. Biol. Chem.* 267:12436–12439.

Zalipsky, S., Brandeis, E., Newman, M. S., and Woodle, M. C. 1994. Long circulating, cationic liposomes containing amino-PEG-phosphatiylethanolamine. *FEBS Lett.* 353:71–74.

Zelphati, O., and Szoka, F. C. Jr. 1996. Intracellular distribution and mechanism of delivery of oligomucleotides mediated by cationic lipid. *Pharm. Res.* 13:1367–1372.

Zelphati, O., Uyechi, L. S., Barron, L. G., and Szoka, F. C. Jr. 1998. Effect of serum components on the physicochemical properties of cationic lipid/oligonucleotide complexes and on their interaction with cells. *Biochim. Biophys. Acta* 1390:119–133.

Effect of Polyethylene Glycol Linker Chain Length of Folate-Linked Microemulsions Loading Aclacinomycin A on Targeting Ability and Antitumor Effect *In vitro* and *In vivo*

Tomonori Shiokawa,[1] Yoshiyuki Hattori,[1] Kumi Kawano,[1] Yukino Ohguchi,[1] Hiroko Kawakami,[2] Kazunori Toma,[2] and Yoshie Maitani[1]

[1]Institute of Medicinal Chemistry, Hoshi University and [2]Noguchi Institute, Tokyo, Japan

ABSTRACT

Purpose: **To establish a novel formulation tumor-targeted drug carrier of lipophilic antitumor antibiotics, aclacinomycin A (ACM), folate-linked microemulsions were prepared and investigated both *in vitro* and *in vivo*.**

Experimental Design: **Three kinds of folate-linked microemulsions with different polyethylene glycol (PEG) chain lengths loading ACM were formulated with 0.24 mol% folate-PEG_{2000}-distearoylphosphatidylethanolamine (DSPE), folate-PEG_{5000}-DSPE, and folate-lipid (without PEG linker) in microemulsions. *In vitro* studies were done in a human nasopharyngeal cell line, KB, which overexpresses the folate receptor (FR), and a human hepatoblastoma cell line, [FR(−)] HepG2. *In vivo* experiments were done in a KB xenograft by systemic administration of folate-linked microemulsions loading ACM.**

Results: **The association of folate-linked microemulsions to KB cells could be blocked by 2 mmol/L free folic acid. Selective FR-mediated cytotoxicity of folate-linked microemulsions loading ACM was obtained in KB but not in HepG2 cells. The association of the folate-PEG_{5000}-linked microemulsion and folate-PEG_{2000}-linked microemulsion with the cells was 200- and 4-fold higher, whereas their cytotoxicity was 90- and 3.5-fold higher than those of nonfolate microemulsion, respectively. The folate-PEG_{5000}-linked microemulsions showed 2.6-fold higher accumulation in solid tumors 24 hours after i.v. injection and greater tumor growth inhibition than free ACM.**

Conclusion: **These findings suggest that a folate-linked microemulsion is feasible for tumor-targeted ACM delivery. This study shows that folate modification with a sufficiently long PEG chain on emulsions is an effective way of targeting emulsion to tumor cells.**

INTRODUCTION

Aclacinomycin A (ACM) hydrochloride is an anthracycline antitumor antibiotic isolated from *Streptomyces galilaeus* MA-144-M1. ACM inhibits synthesis of nucleic acid, especially RNA, by acting as an inhibitor of not only topoisomerase II but also topoisomerase I (1). This drug is widely used for the treatment of stomach, lung, and ovarian carcinoma; malignant lymphoma; and acute leukemia, but its clinical use is still limited by its toxicity. To reduce the toxic responses and increase the antitumor effect of ACM, it should be effectively targeted to the tumor. To achieve this, polyethylene glycol (PEG)–coated (containing PEG-derivatized phospholipid) liposomes, long-circulating liposomes, are promising. ACM is a lipophilic drug that is not stable in water. Therefore, long-circulating microemulsions, which can contain lipophilic agents and have no inner water phase, may be a more suitable carrier for delivery of ACM. We previously reported a long-circulating microemulsion loading ACM that showed successful antitumor effects in animal experiments (2). The antitumor effect would be enhanced by combining long circulation with tumor targeting.

A variety of targeting ligands has been examined as tumor-targeted drug carriers. Folate receptor (FR) is abundantly expressed in a large percentage of human tumors, but it is only minimally distributed in normal tissues (3–6). There are three FR isoforms, α, β, and γ, with distinctive patterns of tissue distribution. FR-α is predominantly expressed in most normal and malignant epithelial tissues (3), FR-β in some nonepithelial malignancies (4, 5), and FR-γ in hematopoietic cells (6). Therefore, FR can serve as an excellent tumor marker as well as a functional tumor-specific receptor.

Folic acid, a high-affinity ligand for FR, retains its receptor-binding and endocytosis properties even if it is covalently linked to a wide variety of molecules. Therefore, the liposomes conjugated to the folate ligand via a PEG spacer have been used to deliver chemotherapeutic agents, oligonucleotide, and markers to receptor-bearing tumor cells, e.g., KB cells, which overexpress FR-α (7–14). Folate-linked microemulsions *in vitro* have also been reported (15), but not yet *in vivo*. From the result of folate-PEG-linked liposomes, it is already known that the length of the PEG linker chain is important for the liposomes to be internalized by recognition of FR (8).

Here, we report the targeting ability and antitumor effect of folate-linked microemulsions, loading ACM both in *in vitro* and *in vivo*, in terms of the PEG length of the folate-PEG linker chain. This study shows that folate modification with a

Received 6/10/04; revised 11/19/04; accepted 12/7/04.
Grant support: Promotion and Mutual Aid Corporation for Private Schools of Japan, Sasakawa Scientific Research Grant from Japan Science Society (Tokyo, Japan), and a Grant-in-Aid for Scientific Research from the Ministry of Education, Culture, Sports, Science and Technology, Japan.
The costs of publication of this article were defrayed in part by the payment of page charges. This article must therefore be hereby marked *advertisement* in accordance with 18 U.S.C. Section 1734 solely to indicate this fact.
Requests for reprints: Yoshie Maitani, Institute of Medicinal Chemistry, Hoshi University, Ebara 2-4-41, Shinagawa-ku, Tokyo 142-8501, Japan. Phone: 81-3-5498-5048; Fax: 81-3-5498-5048; E-mail: yoshie@hoshi.ac.jp.
©2005 American Association for Cancer Research.

sufficiently long PEG chain on emulsions is an effective way of targeting an emulsion to tumor cells.

MATERIALS AND METHODS

Chemicals. PEG_{2000}-distearoylphosphatidylethanolamine (PEG_{2000}-DSPE, mean molecular weight of PEG: M_r 2,000) was supplied, and amino-PEG_{2000}-DSPE and amino-PEG_{5000}-DSPE (mean molecular weight of PEG: M_r 2,000 and 5,000) were kindly donated by NOF Corporation (Tokyo, Japan). ACM hydrochloride for injection (Aclacinon) was kindly donated by Mercian Corporation (Tokyo, Japan). 1,1′-Dioctadecyl-3,3,3′,3′-tetramethylindocarbocyanine perchlorate (DiI) was purchased from Lambda Probes & Diagnostics (Graz, Austria). Folic acid, cholesterol, and vitamin E were purchased from Wako Pure Chemical Industries, Ltd. (Osaka, Japan). Other reagents used in this study were reagent grade.

Synthesis of the Folate-Lipid and Folate-Polyethylene Glycol-Lipid. Folate-lipid (direct folate conjugate of lipid), *N*-(*N*-folyl-6-aminohexyl)-3,5-bis(dodecyloxy)benzamide, was synthesized as follows (Fig. 1*A*). Folic acid (300 mg, 0.680 mmol) and dicyclohexylcarbodiimide (280 mg, 1.36 mmol) were dissolved in DMSO/pyridine (10 mL/4 mL) and the solution was stirred at room temperature for 1 hour. *N*-(6-Aminohexyl)-3,5-bis(dodecyloxy)benzamide (400 mg, 0.680 mmol; ref. 16) was added to the solution and the reaction was continued at room temperature for another 3 hours. The resulting mixture was concentrated to remove pyridine and cooled at 4°C. The resulting precipitate was collected by filtration and was washed with methanol to give *N*-(*N*-folyl-6-aminohexyl)-3,5-bis(dodecyloxy)benzamide (412 mg, 0.407 mmol) at a yield of 60%. ^{1}H nuclear magnetic resonance (600 MHz, DMSO-d_6/D_2O = 98:2) δ0.85 (6H, t, J = 6.9 Hz), 1.20 to 1.32 (36H, m), 1.39 (6H, m), 1.49 (2H, m), 1.69 (4H, quint, J = 6.8 Hz), 1.88 (1H, m), 1.99 (1H, m), 2.25 (2H, t, J = 7.9 Hz), 3.05 (2H, m), 3.20 (2H, m), 3.97 (4H, t, J = 6.8 Hz), 4.35 (1H, dd, J = 3.9, 3.4 Hz), 4.48 (2H, s), 6.56 (1H, s), 6.65 (2H, d, J = 8.6 Hz), 6.95 (2H, s), 7.64 (2H, d, J = 8.6 Hz), 8.64 (1H, s).

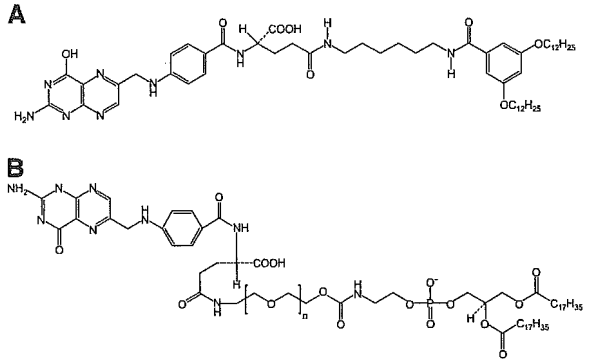

Fig. 1 Structure of the folate-linked lipids. *A,* folate-lipid, which is a folate direct conjugate of a double-chain lipid, was synthesized by dicyclohexylcarbodiimide-mediated coupling. *B,* folate-PEG_{5000}-DSPE and folate-PEG_{2000}-DSPE, which are conjugates of folate and PEG-DSPE, were also synthesized by dicyclohexylcarbodiimide-mediated coupling of folic acid to amino-PEG-DSPE. n ≈ 42 (PEG_{2000}), 113 (PEG_{5000}).

Folate-linked PEG_{2000}-DSPE (folate-PEG_{2000}-DSPE) and folate-PEG_{5000}-DSPE, which are conjugates of folic acid and amino-PEG-DSPE, were prepared as previously reported (Fig. 1*B*; ref. 8). The folate content of the product was determined by quantitative UV spectrophotometry of the product dissolved in a 10 mmol/L Tris-HCL buffer (pH 8.0) / methanol (1:1, v/v) at 285 nm. The yields of folate-PEG_{2000}-DSPE and folate-PEG_{5000}-DSPE were 86% and 75%, respectively. The chemical structure of the product was analyzed by electrospray ionization time-of-flight mass spectrometry. Electrospray ionization-ion trap mass spectrometry (methanol) calculated for $C_{155}H_{288}N_9O_{62}P$ (n = 46), $[M\text{-}2H]^{2-}/2$ 1,649.5, found 1,648.3; calculated for $C_{157}H_{292}N_9O_{63}P$ (n = 47), $[M\text{-}2H]^{2-}/2$ 1,671.5, found 1,669.8; calculated for $C_{159}H_{296}N_9O_{64}P$ (n = 48), $[M\text{-}2H]^{2-}/2$ 1,693.5, found 1,692.3.

Preparation of Microemulsions. Microemulsions were composed of PEG_{2000}-DSPE/cholesterol/vitamin E/ACM hydrochloride (M-ACM, 3:3:3:1, weight ratio; 7:48.3:43.3:1.5, molar ratio). Drug-free folate-linked microemulsions are expressed as F/M. Folate-PEG_{5000}-DSPE (F5), folate-PEG_{2000}-DSPE (F2), and folate-lipid (F0), at a mol% of 0.24, were added as a part of PEG_{2000}-DSPE of M-ACM (F5, F2, F0/PEG_{2000}-DSPE/cholesterol/vitamin E/ACM hydrochloride = 0.24:6.7:48.3:43.3:1.5, molar ratio; F5/M-ACM, F2/M-ACM, F0/M-ACM, respectively). Microemulsions were prepared by a modified ethanol injection method as described previously (2), except for F0/M-ACM. For F0/M-ACM, folate-lipid and cholesterol were dissolved in an appropriate volume of chloroform that was then removed. The subsequent process after being dissolved in ethanol was the same as for the other microemulsions. DiI-labeled F5/M, F2/M, F0/M, and microemulsion were prepared by the same protocol, but with post-addition of DiI at 1.33 mol% of the total lipids. The particle diameter distribution of microemulsions was measured by the dynamic light scattering method with ELS-800 (Otsuka Electronics Co., Ltd., Osaka, Japan) at 25°C by diluting the dispersion to an appropriate volume with water. The ACM-loading efficiency was taken as the percentage of ACM carried by the microemulsions and was determined by Sephadex G-50 chromatography and a fluorescence detector, as described previously (2). The ACM-loading efficiency was also confirmed by measuring the ACM amount of the microemulsion fraction using high-performance liquid chromatography as described in Biodistribution Studies in Tumor-Bearing Mice.

Cell Culture. KB cells were obtained from the Cell Resource Center for Biomedical Research, Tohoku University (Miyagi, Japan). HepG2 cells were obtained from the Riken Cell Bank (Ibaraki, Japan). Both cells were cultured in folate-deficient MEM (originally prepared based on Eagle's MEM) with 10% heat-inactivated fetal bovine serum (Invitrogen Corp., Carlsbad, CA) and 50 μg/mL kanamycin sulfate (Wako Pure Chemical Industries) as a 5% CO_2 at 37°C.

RNA Isolation and Reverse Transcription-PCR. Total RNA was isolated from KB and HepG2 cells, respectively, using NusleoSpin RNA II (Macherey-Nagel, Dueren, Germany). RNA yield and purity were checked by spectrometric measurement at 260 and 280 nm and RNA electrophoresis, respectively. First-strand cDNA was synthesized from 5 μg total RNA after denaturation for 5 minutes at 65°C using 50 pmol random primer, 0.5 mmol/L deoxynucleotide triphosphate, and 5 units

of AMV Reverse Transcriptase XL (Takara Shuzo Co., LTD., Japan). The reaction was done at 41°C for 1 hour in 20 μL volume. For reverse transcription-PCR, a 25 μL reaction volume contained the following: 1 μL synthesized cDNA, 10 pmol of each specific primer pair, and 0.25 units Ex Taq DNA polymerase (Takara Shuzo) with a PCR buffer containing 1.5 mmol/L $MgCl_2$ and 0.2 mmol/L of each deoxynucleotide triphosphate. The profile of PCR amplification consisted of denaturation at 94°C for 0.5 minute, primer annealing at 58°C for 0.5 minute, and elongation at 72°C for 1 minute for 25 cycles. PCRs of the housekeeping gene *β-actin*, *FRs* (*FR-α*, *FR-β*, *FR-γ*), and *reduced folate carrier* were done at the same cycle run for all samples. The PCR products for FRs, reduced folate carrier, and β-actin were analyzed by 1.5% agarose gel electrophoresis in a Tris-borate-EDTA buffer. The products were visualized by ethidium bromide staining.

Flow Cytometry Analysis. Cells were prepared by plating 3×10^5 cells in a 12-well culture plate 1 day before the assay. Cells were incubated with DiI-labeled microemulsions [F5/M, F2/M, F0/M, and microemulsion (M-ACM without ACM) containing 90 μg total lipid] diluted in 1 mL serum-free medium for 1 hour at 37°C. In free folate competition studies, 2 mmol/L folic acid was added to the medium. After incubation, cells were washed thrice with cold PBS (pH 7.4) to remove unbound microemulsions, detached with 0.02% EDTA-PBS, and then suspended in PBS containing 0.1% bovine serum albumin and 1 mmol/L EDTA. The suspended cells were directly introduced to a FACSCalibur flow cytometer (Becton Dickinson, San Jose, CA) equipped with a 488 nm argon ion laser. Data for 10,000 fluorescent events were obtained by recording forward scatter, side scatter, and 585/42 nm fluorescence. The autofluorescence of cells was taken as a control; cells were incubated with serum-free medium without drugs for 1 hour.

Confocal Microscopy. Cell cultures were prepared by plating 3×10^5 cells in 35 mm culture dishes 1 day before the experiment. Medium was replaced with 1 mL fresh serum-free medium containing either F2/M-ACM or M-ACM (containing 0.5 μg ACM/mL). Following 1-hour incubation, each dish was rinsed five times with 1 mL cold PBS and then fixed with 1 mL 20% neutral-buffered formalin (Mildform 20 N, Wako Pure Chemical Industries) for 1 hour at room temperature. Cell-associated fluorescence was imaged using a Radiance 2100 confocal laser-scanning microscope (Bio-Rad Laboratories, Inc., Hercules, CA). Maximum excitation was done with the 488 nm line of an argon laser and fluorescence emission was observed at >570 nm (using 560DCLP and E570LP filters).

Cytotoxicity Study. Briefly, 5×10^4 cells were plated into 96-well culture plates 1 day before the experiment. KB and HepG2 cells were then incubated for 1 hour at 37°C with 100 μL F5/M-ACM, F2/M-ACM, M-ACM, or free ACM (containing 0.004, 0.04, 0.4, or 4 μg ACM) diluted in 1 mL serum-free medium. The medium was then replaced with fresh medium and incubated for a further 72 hours. The cytotoxicity was determined by a WST-8 assay (Cell Counting Kit-8, Dojindo Laboratories, Kumamoto, Japan). The number of viable cells was then determined by absorbance measured at 450 nm on an automated plate reader.

***In vitro* Drug Release.** The release of the drug in M-ACM in PBS (pH 7.4) was monitored by a dialysis method. The dialysis was done at 37°C using seamless cellulose tube membranes (Viskase Sales Corp., Willowbrook, IL) with molecular weight cutoff of M_r 14,000 as the sink solution. The initial concentration of M-ACM was 20 μg/mL. The sample volume in the dialysis bag was 1 mL and the sink volume was 100 mL. The concentration of drug was analyzed at various time points during the dialysis process. The concentration of drug was monitored using high-performance liquid chromatography as described in Biodistribution Studies in Tumor-Bearing Mice.

Animals and Inoculation of Tumor Xenografts. Specific pathogen-free female athymic BALB/c *nu/nu* nude mice (7 weeks of age on arrival, Oriental Yeast Co., Ltd., Tokyo, Japan) were maintained on a folate-deficient diet (AIN-93M-based Folate-Deficient Rodent Diet, Oriental Yeast) on arrival and for the duration of the study. To generate tumor xenografts, a KB cell suspension of appropriate concentration in PBS was injected s.c. in the right hind crus of the mice. The animal experiments were done under ethical approval from our Institutional Animal Care and Use Committee.

Serum Folate Concentration. Tumor-inoculated mice were first maintained on a regular diet (MF Rodent Certified Diet, Oriental Yeast) for 3 weeks on arrival and then either continued on this diet or switched to a folate-deficient diet for 1 week. Folate concentration in sera was measured using a competitive enzyme immunoassay kit, AIA-Pack Folate (Tosoh Corporation, Tokyo, Japan).

Biodistribution Studies in Tumor-Bearing Mice. Mice were s.c. inoculated with 2×10^6 cells and then grouped at random. Seven days after inoculation, mice were given F5/M-ACM, M-ACM, and free ACM by i.v. injection via the lateral tail vein at a single dose of 5 mg ACM/kg. After 24 hours, the mice were anesthetized by ether inhalation and immediately sacrificed by cervical dislocation. Blood was collected in heparinized tubes and immediately centrifuged to separate plasma from blood cells. The liver, spleen, kidneys, heart, lung, and tumor were removed, rinsed in physiologic saline, weighed, and frozen at −20°C. They were homogenized by adding 0.2 mol/L phosphate buffer (pH 7.0). ACM was extracted from the biological samples as previously reported (17). The high-performance liquid chromatography system was composed of an LC-10AS pump (Shimadzu Co., Ltd., Kyoto, Japan), an RF-10AXL fluorescence detector (excitation = 435 nm, emission = 505 nm; Shimadzu), and a YMC-Pack ODS-AA-302 column (150 × 4.6 mm internal diameter, YMC Co., Ltd., Kyoto, Japan). The mobile phase was acetonitrile/methanol/1.5% aqueous H_3PO_4 (40:90:70, v/v) and the flow rate was 1.0 mL/min (18). The concentration of ACM in each sample was determined using a calibration curve.

Antitumor Effects. To evaluate the antitumor effects of microemulsion, mice were inoculated with 1×10^6 cells s.c. in the hind crus and were then grouped at random (day 0). Three days after inoculation, treatment was started at a dose of 5 mg ACM/kg: (*a*) F5/M-ACM, (*b*) F2/M-ACM, (*c*) M-ACM, (*d*) free ACM, and (*e*) saline as a control. The drugs were administered by i.v. injection via the lateral tail vein on every 3rd day (on day 3, 6, 9, 12, and 15). Tumor size was measured with vernier calipers on every 3rd day eight times (on day 3, 6, 9, 12, 15, 18, 21, and 24). Tumor volume was